UNIVERSITÄT BERN

New materials enabling alternative energy technologies

Anke Weidenkaff,
Solid State Chemistry and Catalysis, Empa,
University of Bern, CH-3012 Bern, Switzerland

Empa, Swiss Federal Laboratories for Materials Research and Technology

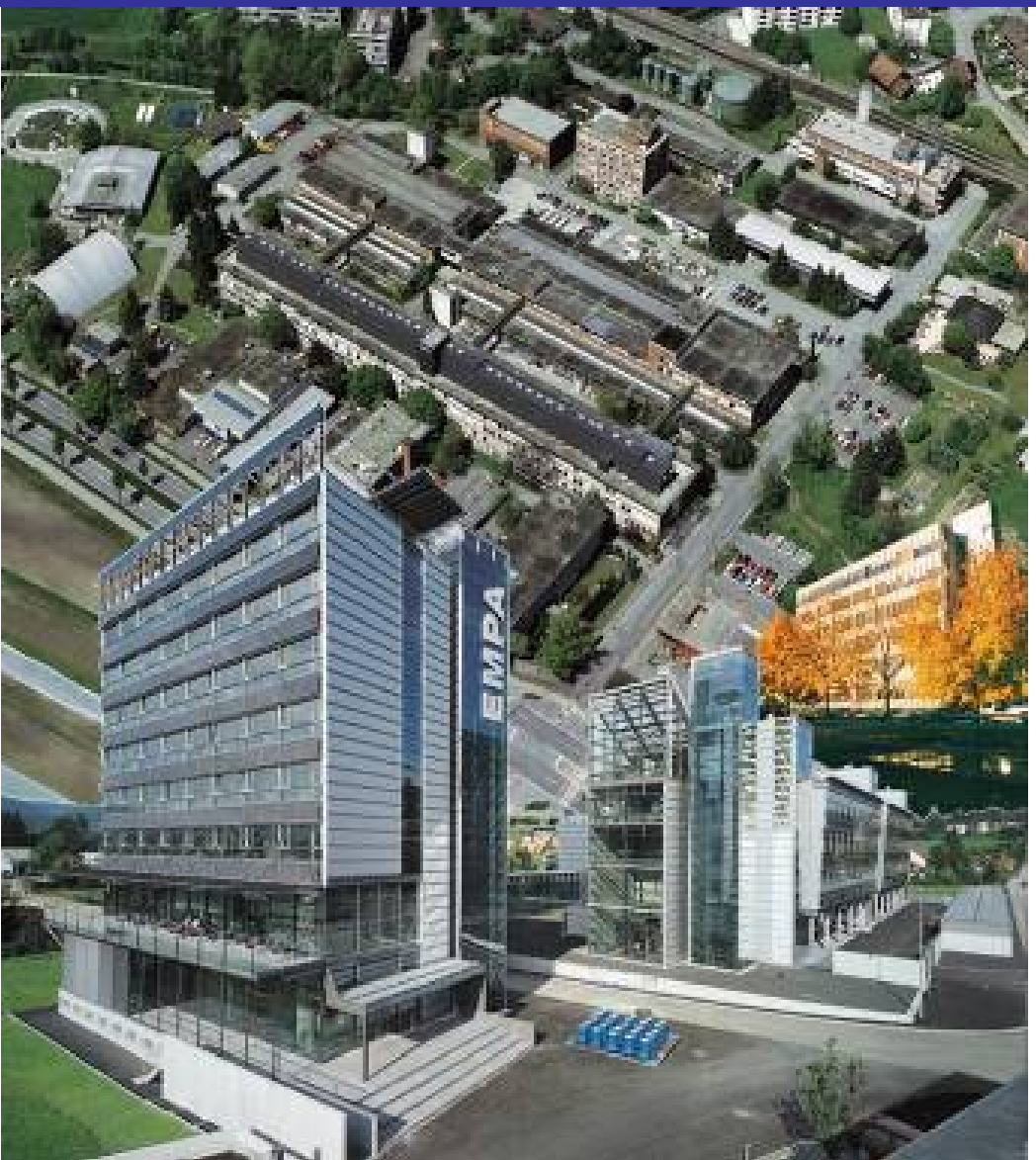

3 Sites

Zürich-Dübendorf, St. Gallen, Thun

950 Employees

400	University graduates including 190 PhDs
100	Graduates of universities of applied science
130	PhD students
9	Professors

Budget

90 mill. CHF federal funding
32 mill. CHF third party funding
13 mill. CHF services

Empa's Research Focal Areas

Materials for health and performance

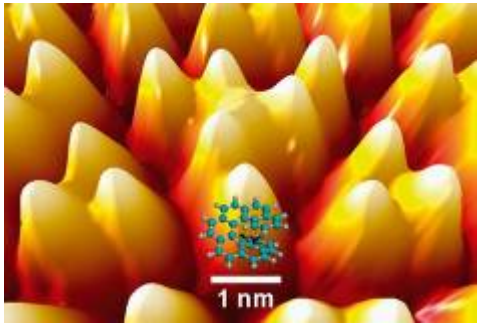

Nanotechnology

Adaptive materials and systems

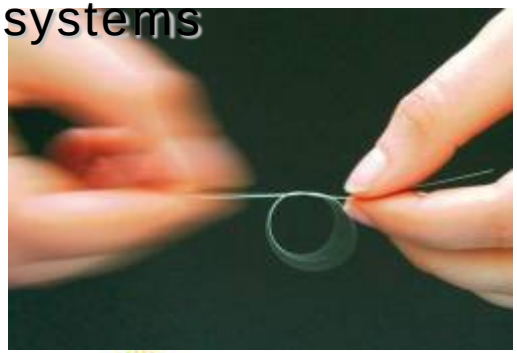

Natural Resources and Pollutants

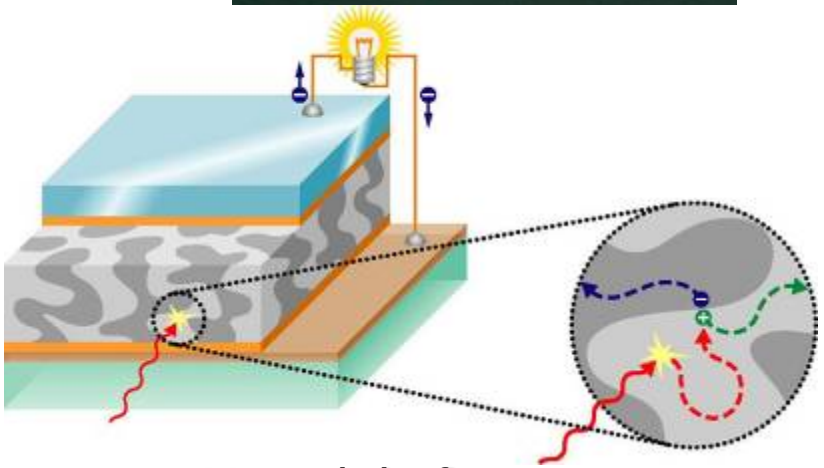

Materials for energy technologies

Materials Design for Energy Converters: Solid State Chemistry

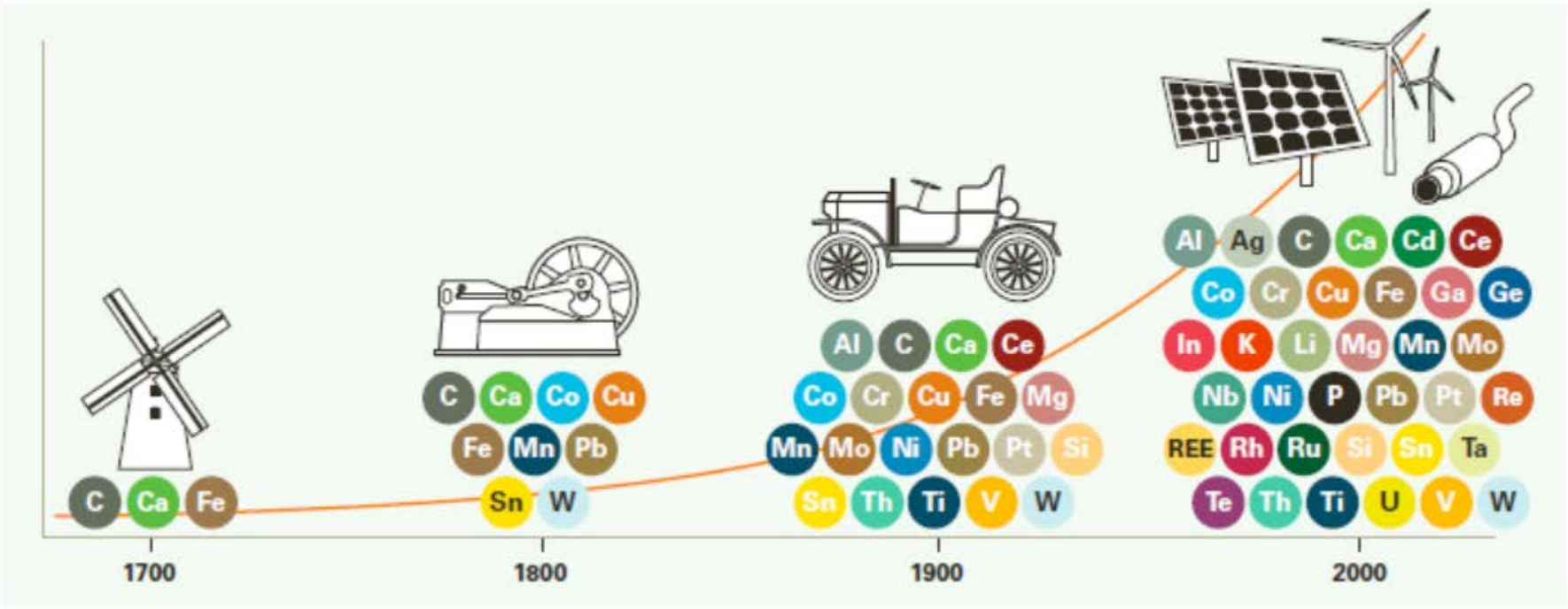

Tailoring of Materials and Functions: Structure-composition-property relationship

- **3D's** Approach**:** **D**oS (Theory, band structure design),
  Defects (*Realstruktur*) and **D**imensionality (form and architecture)
  Dynamics (reactivity, regenerative materials for reversible processes, e.g. rechargeable battery)

Advanced Materials for Future Energy/Mobility Technologies

- Solar energy technologies
- New solar fuels: H_2/CH_4
- E- and CNG- mobility
- Efficiency

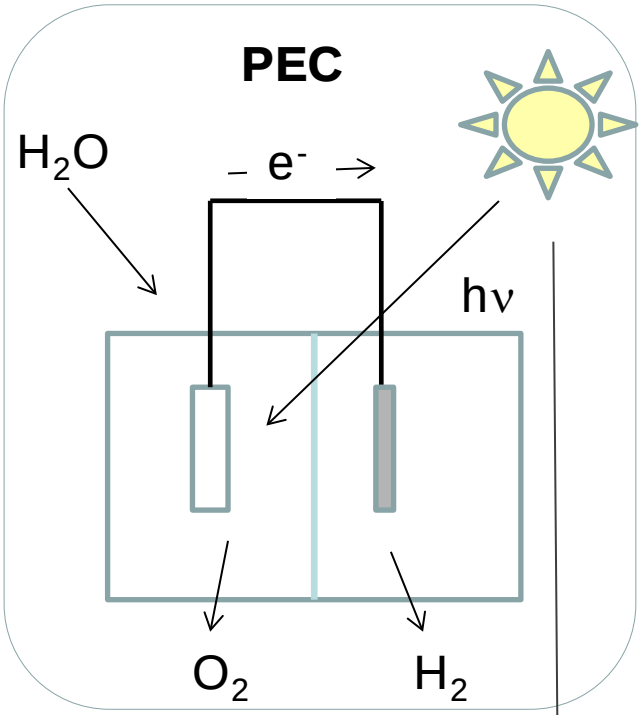

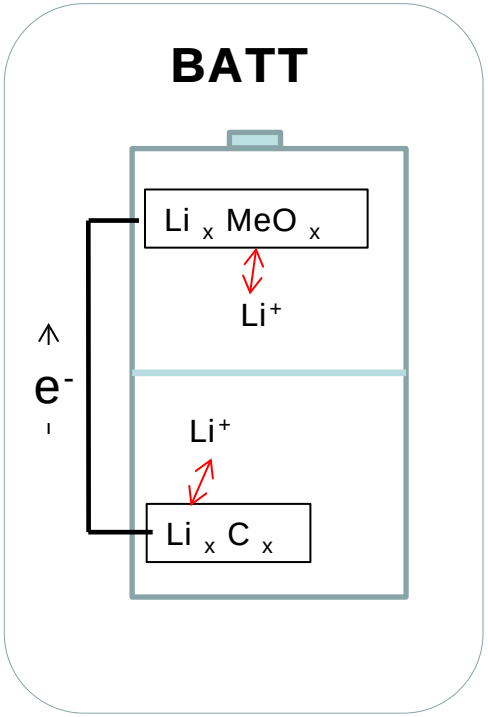

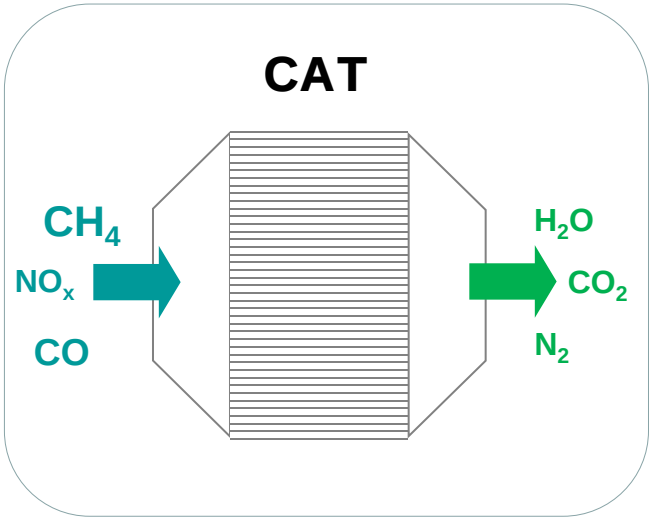

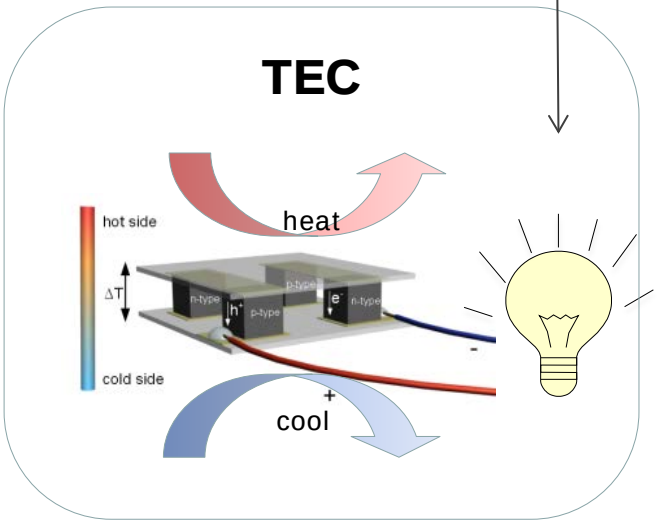

EMPA

Materials Science & Technology

Outline

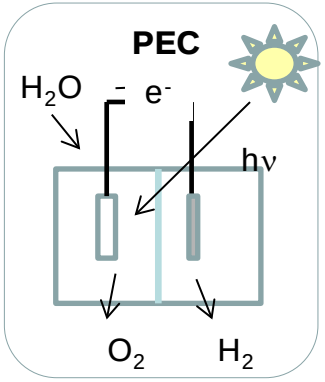

0.) Materials Design by 3D's, perovskites

1.) Solar H_2 by photoelectrochemistry

- ✓ Oxynitrides capture sunlight efficiently: appropriate E_g
- ✓ high catalytic activity: suitable surface of nanocrystallites

→ Gas evolution: 100 mg from 12 to >43 μmole/h

→ PEC: enhanced intergrain connectivity increases photocurrent

2.) High temperature Solar Thermoelectric converters

- ✓ chemical stability in air up to 1000K: Carnot ↗, energy density ↗
- ✓ large thermopower in good conductors: correlated electronic systems
- ✓ Phonon backscattering
- ✓ Thermoelectric oxides

  → from ZT<<0.1 to ZT > 0.4 to convert concentrated solar radiation.

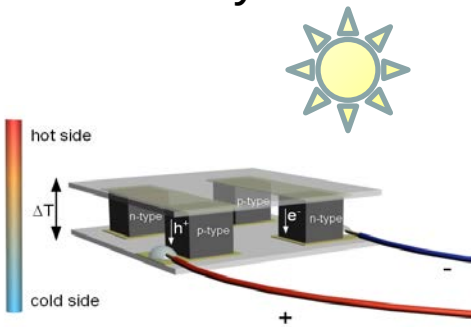

Tailoring of thermoelectric, catalytic and electrochemical materials

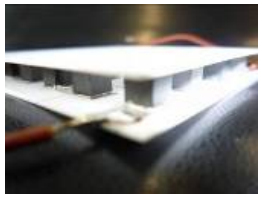

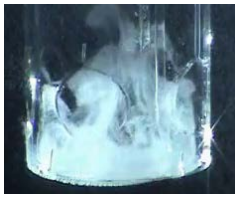

>1W/cm^2 >0.1 mol/h

test

applications
- thermoelectricity, catalysis, batt.
- requirements: transp.prop., regenerativity, ..

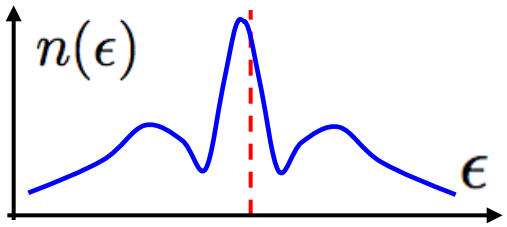

theory (3 D's)
economy,
ecology

characterisation
- DoS, structure, comp.
- Defect structure
- Dynamic behavior

materials choice
- perovskites-type oxides and oxynitrides
- heusler compounds

function, form, scalability

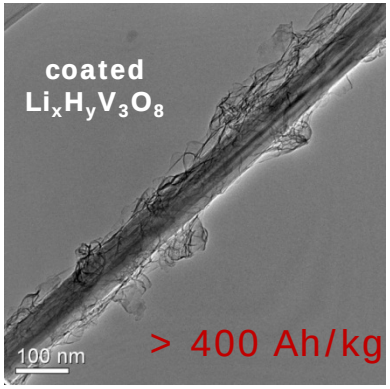

synthesis
- "chimie douce",
- USC, flame spray
- Single Crystals

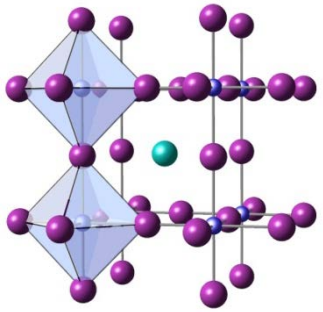

EMPA
Materials Science & Technology

Outline

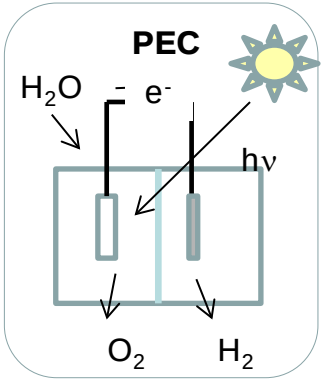

0.) Materials Design by 3D's, perovskites

1.) Solar H_2 by photoelectrochemistry

- ✓ Oxynitrides capture sunlight efficiently: appropriate E_g
- ✓ high catalytic activity: suitable surface of nanocrystallites

→ Gas evolution: 100 mg from 12 to >43 μmole/h

→ PEC: enhanced intergrain connectivity increases photocurrent

2.) High temperature Solar Thermoelectric converters

- ✓ chemical stability in air up to 1000K: Carnot ↗, energy density ↗
- ✓ large thermopower in good conductors: correlated electronic systems
- ✓ Phonon backscattering
- ✓ Thermoelectric oxides

  → from ZT<<0.1 to ZT > 0.4 to convert concentrated solar radiation.

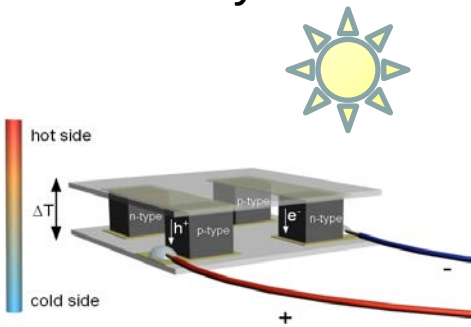

1.) Solar H_2 by photoelectrochemistry

NanoPEC

Development of better photocatalysts

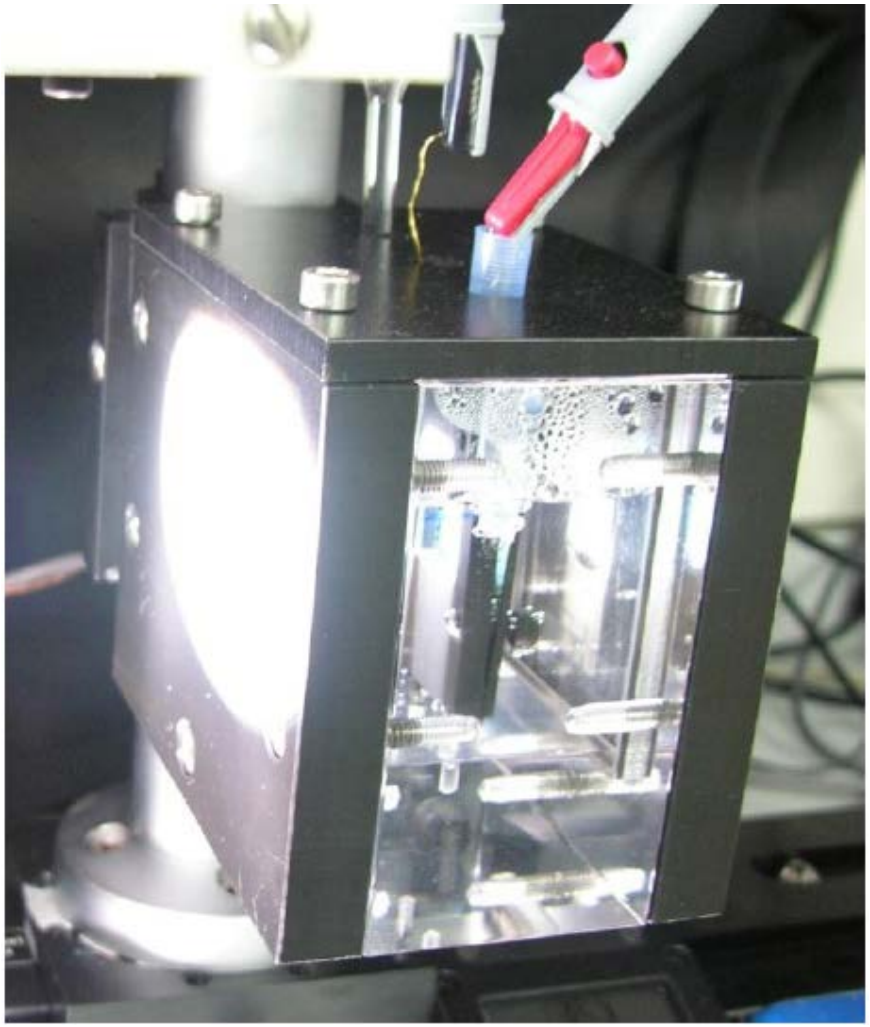

http://nanopec.epfl.ch

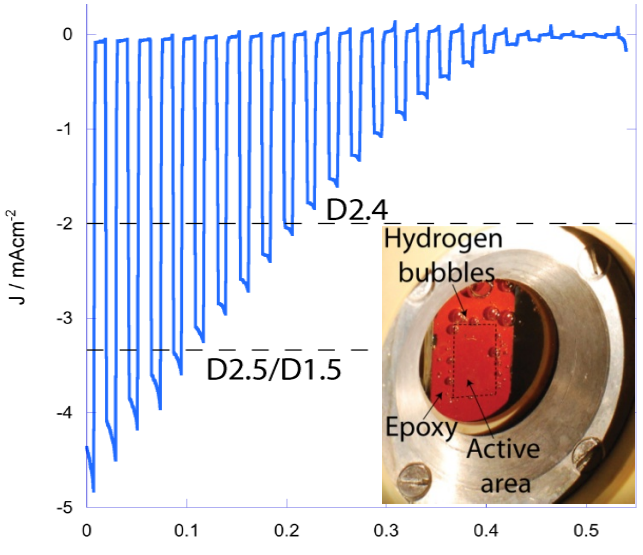

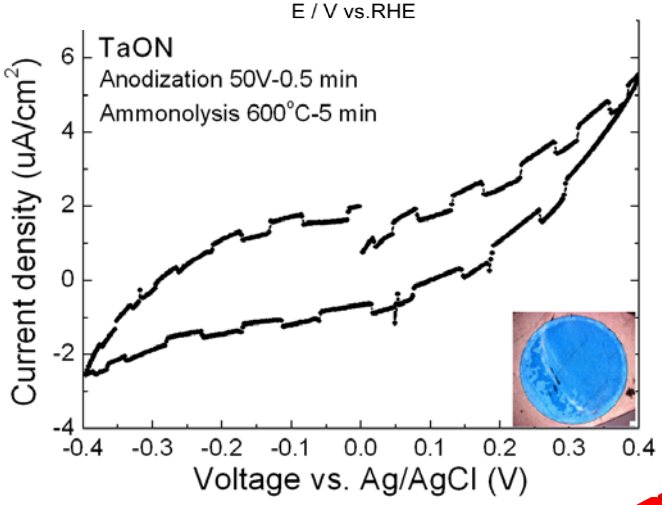

EMPA

A. Mägli (Empa), M. Graetzel (EPFL), L. Meda (ENI), A. Rothschild (Technion), R. van de Krol (Delft), ...

ence & Technolog y

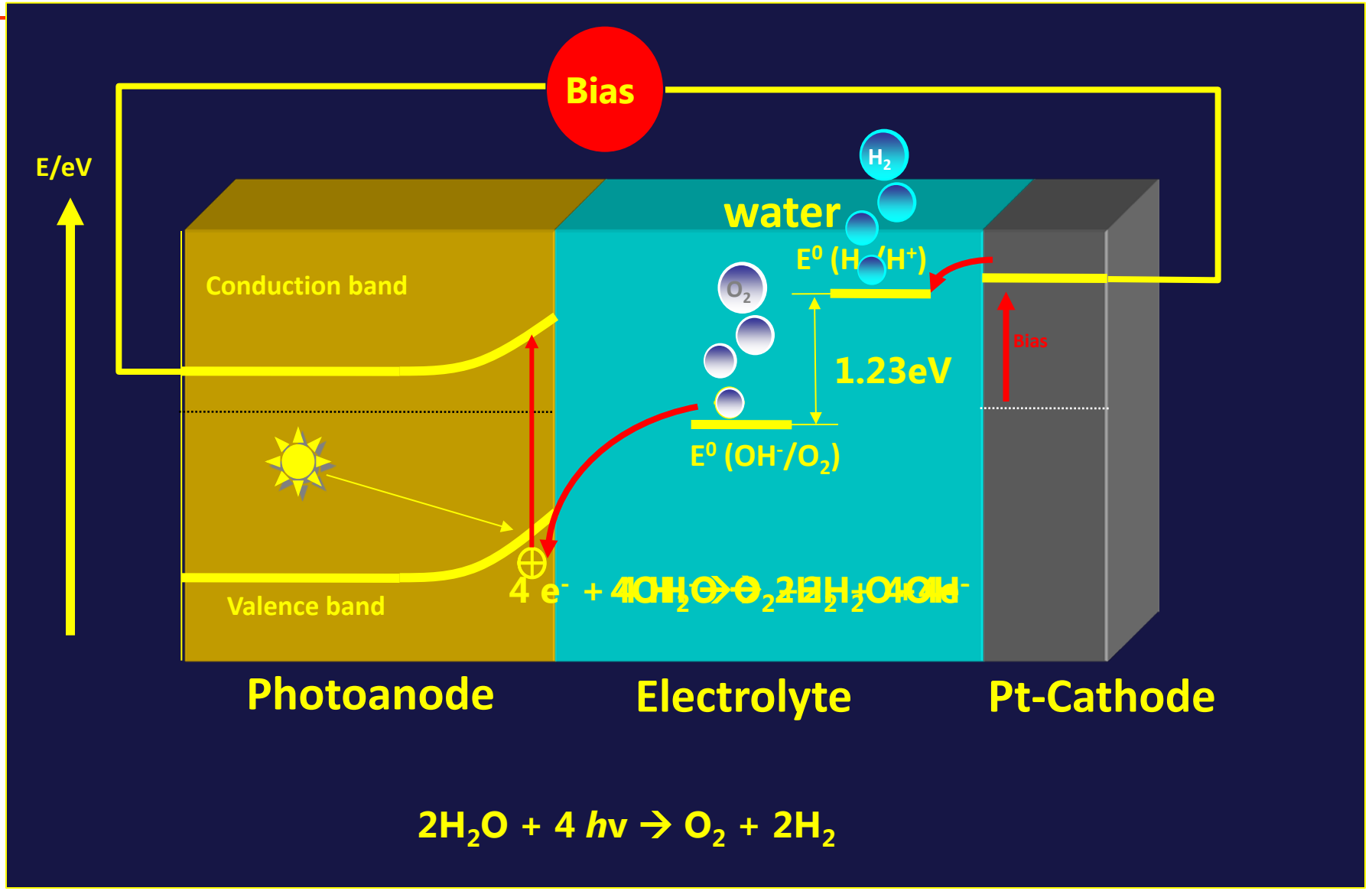

http://nanopec.epfl.ch

EMPA
Materials Science & Technology

Band position tuning of semiconductors in contact with aqueous electrolyte

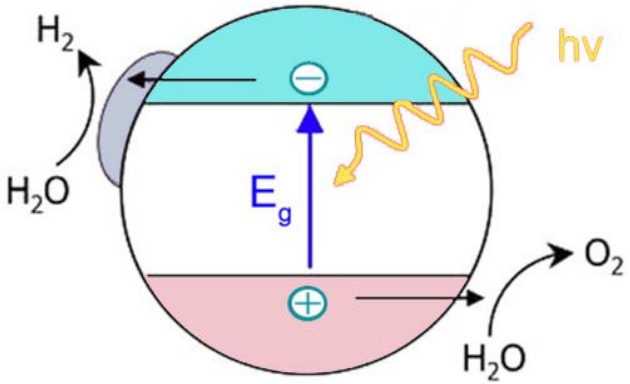

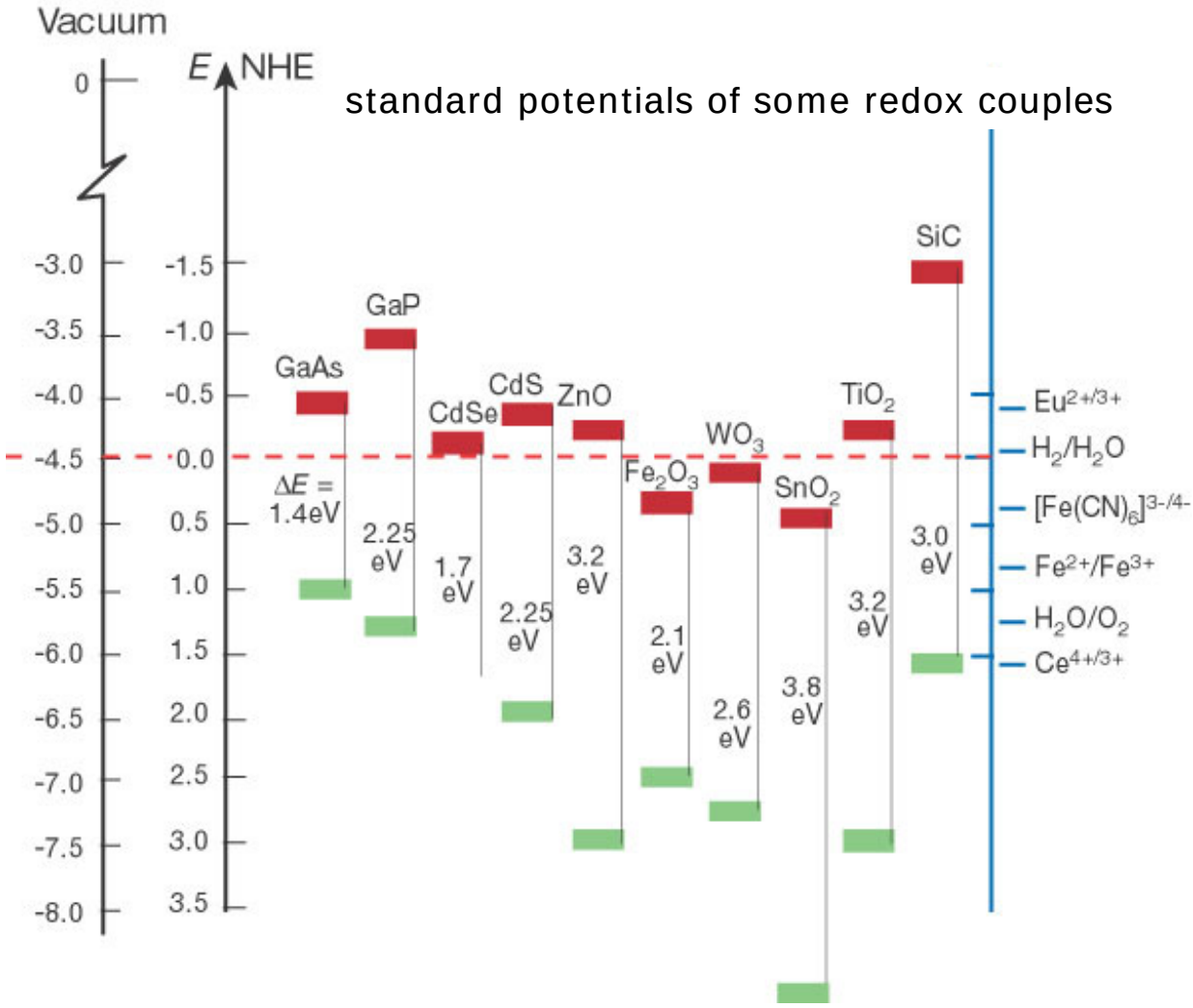

(NHE) normal hydrogen electrode
lower edge of the conduction band (red colour)
upper edge of the valence band (green colour)

M. Grätzel et al., *Nature* **414** (2001)338

Perovskites: One structure, many properties

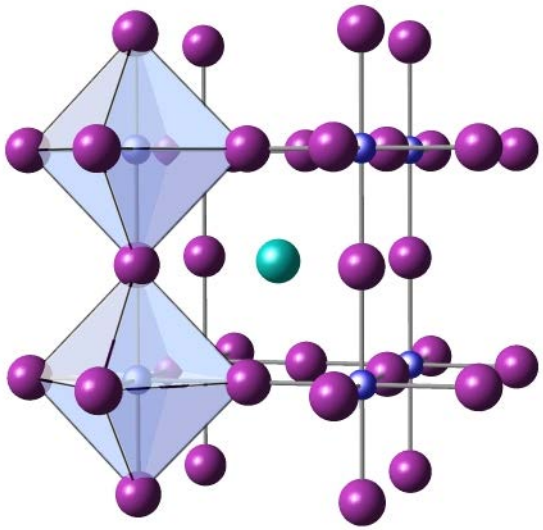

ABX_3

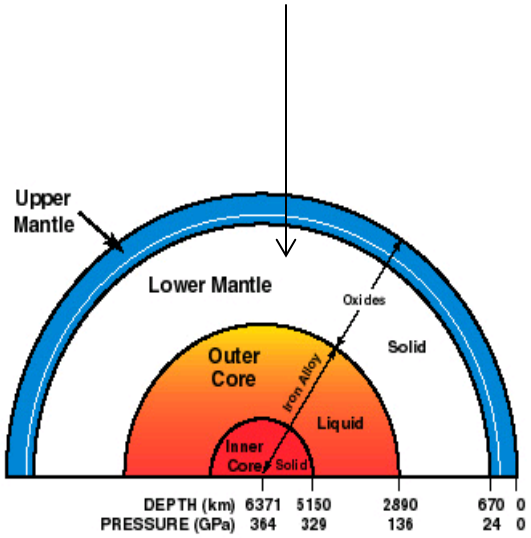

- $(Mg,Fe)SiO_3$ is the most abundant mineral in the lower earth mantel
- One stable structure type with highly diverse chemical compositions, attractive band structures and techn functions
- Correlated electronic system, spin entropy, DoS / band gap management
- Stable distorted structures, super structures, layered structures, polar structures, defects
- A– cation deficient, B– cation deficient, Anion deficient
- Non-stoichiometric regenerative compounds
- Applications: High-κ dielectrics for capacitors, microwaves, high frequency telecommunication, pyroelectric detectors, HTSC based electronics, spintronics, thermoelectrics, FC catalysts, exhaust gas catalysts …

Chimie douce synthesis methods

Complexing cations

Polymerization for 3h at 353 K

viscous gel

Predrying stage at 423 K

xerogel

Diff.

- Low T synthesis (T < 900K)
- Submicrometer particles
- Fast & low cost process

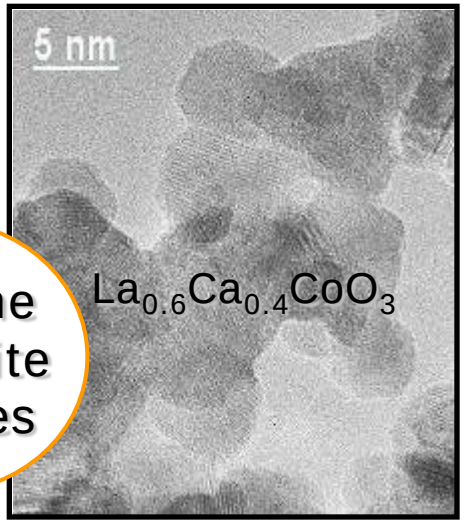

Thin films

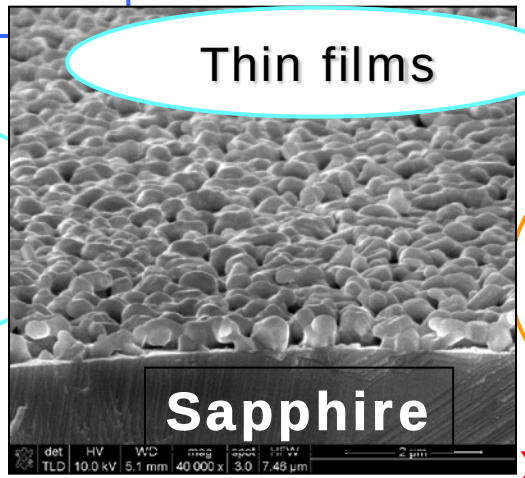

Pellets by hot pressing, MW, SPS

Ultra fine perovskite particles

electr. and heat transport, application test

XRD, ND, XAS, TEM, TGA

Synthesis methods for low D mat.

- Chimie douce, micelles, sol-gel, …
- Ultrasonic and flame spray combustion
- Microwave induced plasma: heterostructures and core-shell particles

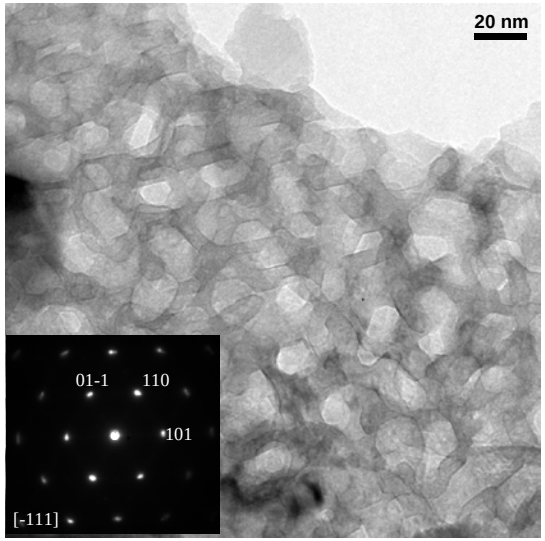

Mesoporous $(La,Sr)TiO_3$

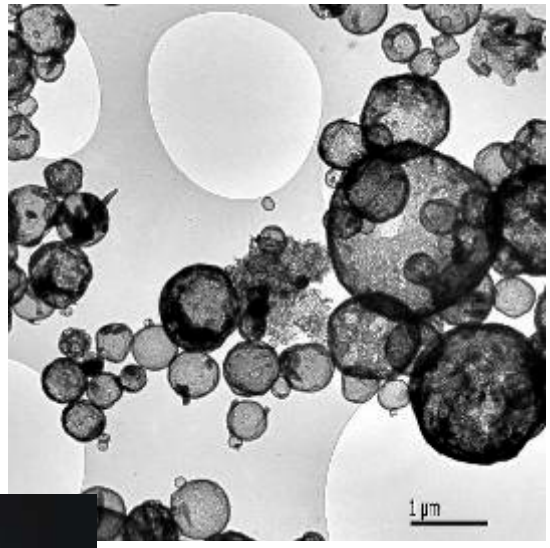

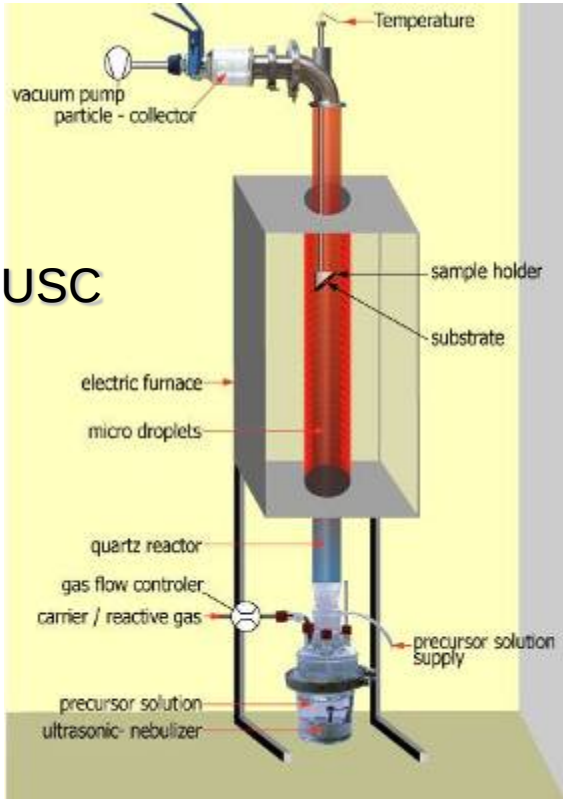

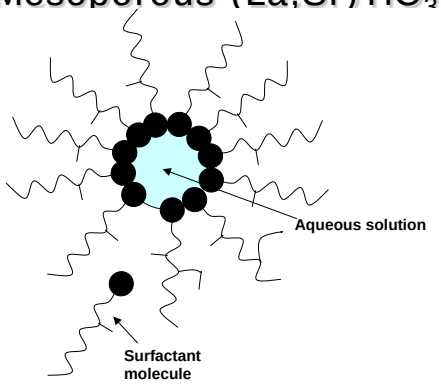

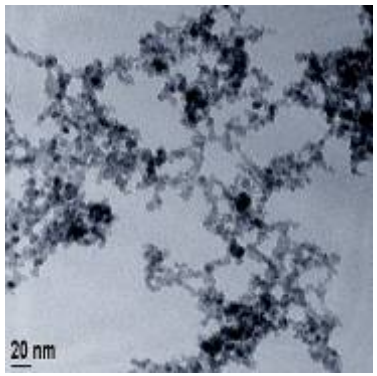

Oxynitrides: Anionic substitutions in perovskite-type phases

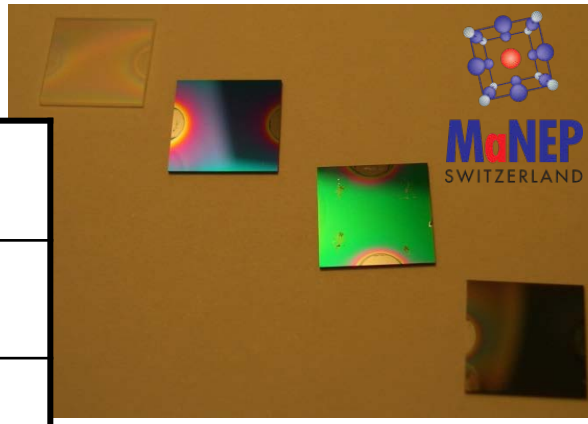

Suitable ions to substitute oxygen in perovskites

Ion	S^{2-}	N^{3-}	O^{2-}	Cl^{-}	F^{-}
r (C.N.=6), nm	1.84	1.50	1.40	1.81	1.33
χ	2.60	3.07	3.50	2.83	4.10
Electronic configuration	$3s^23p^6$	$2s^22p^6$	$2s^22p^6$	$3s^23p^6$	$2s^22p^6$

- Structural investigations on perovskite-type oxynitrides are rare
- mainly polycrystalline samples are described
- Physical properties are inadequately characterised until now

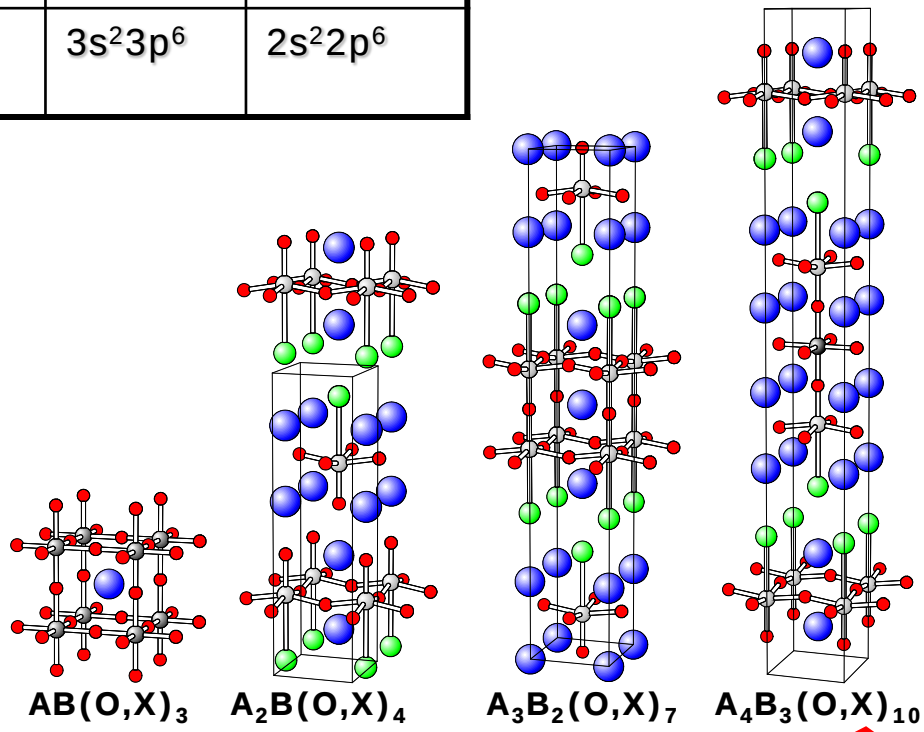

EMPA
Materials Science & Technology

O/N substitution in perovskite-type materials: Band structure

$$La_2Ti_2O_7 + 2\ NH_3 \rightarrow 2\ LaTiO_2N + 3\ H_2O$$

+ NH_3

Thin slice of $LaTiO_{3.5}$ crystal

Thin slice after ammonolysis $LaTiO_2N$

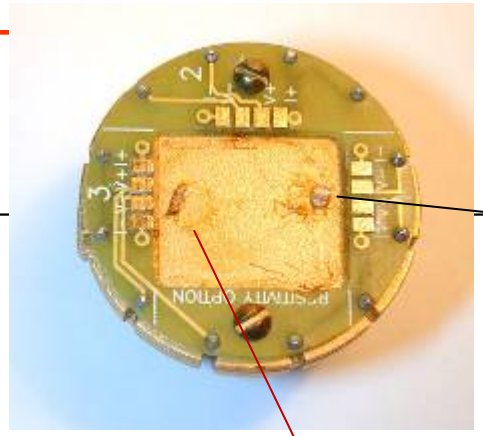

$Ca_{1-x}La_xTa_{1-y}Ti_yO_{2-z}N_{1+z}$

Jansen, M. and H. P. Letschert (2000). "Inorganic yellow-red pigments without toxic metals." Nature **404** (6781): 980-982.

Aguiar, R., Logvinovich, D., Weidenkaff, A., Reller , A., Ebbinghaus, S.G., The vast colour spectrum of ternary metal oxynitride pigments, *Dyes and Pigments*, **76** (2008) 70-75

EMPA

Materials Science & Technology

Oxynitrides as visible-light driven photocatalysts

- χ (Nitrogen) < χ (Oxygen): smaller bandgap E_g compared to oxide counter-parts
  → Efficient utilisation of solar spectrum due to visible light absorption

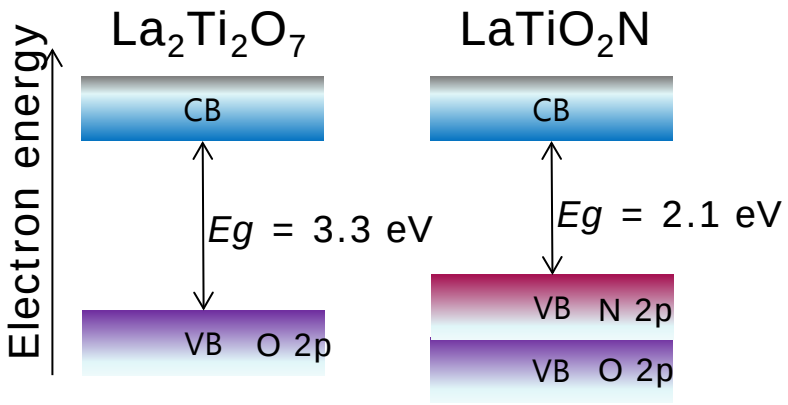

[3] H. Zhou *et al.*, Energy Environ. Sci, 2012, 5.

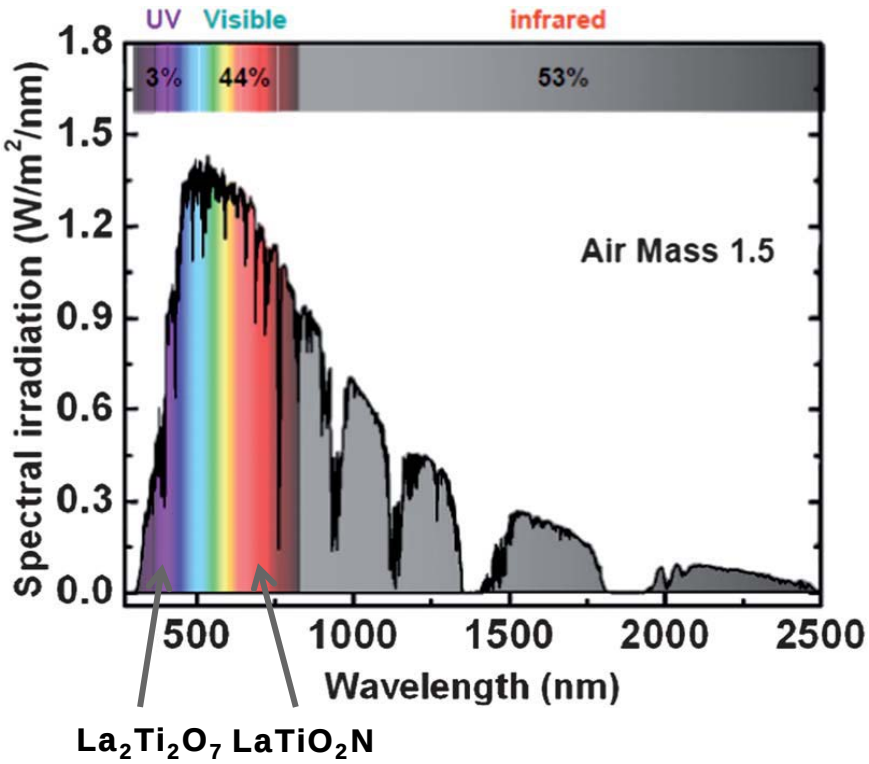

Aguiar, R., Lee, Y., Domen, K., Kalytta, A., Logvinovich, D., Weidenkaff, A., Reller, A., Ebbinghaus, S.G, *Ceram. Res. Adv.*, ISBN: 1-60021-769-9 (2007).

EMPA
Materials Science & Technology

Band gap tuning of perovskite-type oxynitride niobates

$LaNbON_2$	$BaNbO_2N$	$SrNbO_2N$	$CaNbO_2N$
orthorhombic	Cubic	Tetragonal	orthorhombic
Nb-(O,N)-Nb = 160°	Nb-(O,N)-Nb = 180°	Nb-(O,N)-Nb = 173°	Nb-(O,N)-Nb = 153°
Gap 1.7 eV	Gap 1.8 eV	Gap 1.9 eV	Gap 2.1 eV

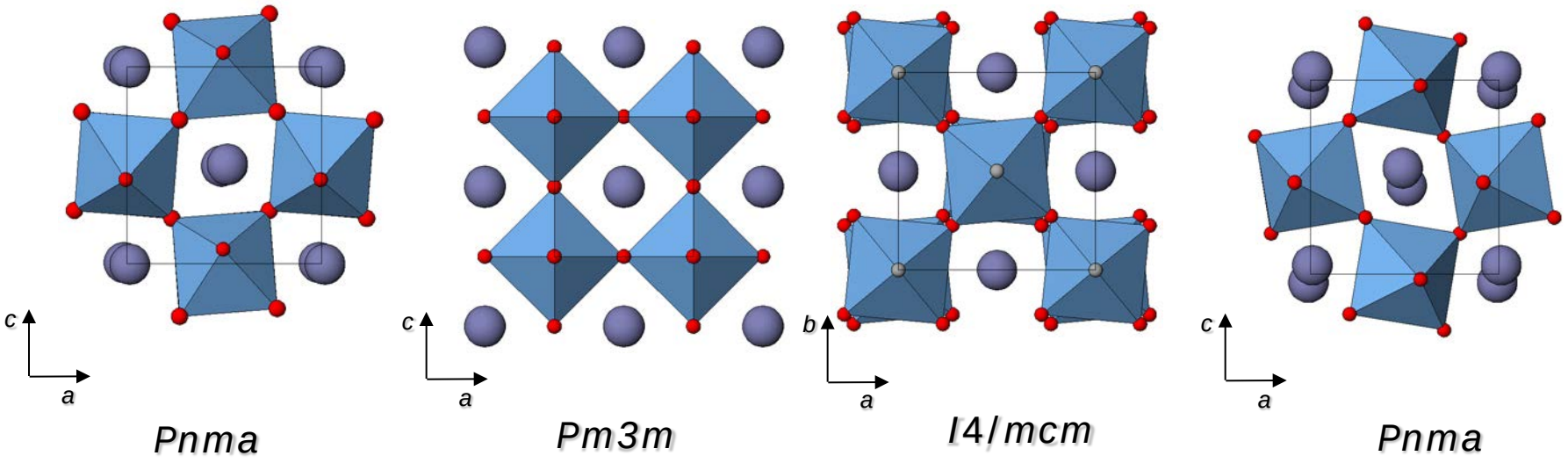

Ionic radii : Ba (1.61 A) > Sr (1.41 A) > La (1.18 A) > Ca (1.12 A)

Logvinovich, D., Börger, A., Döbeli, M., Ebbinghaus, S.G., Reller, A. and Weidenkaff, A, Progr. in Solid State Chem., 35 (2007) 281-290.

Morphology, *Realstruktur* of $LaNbO_{1.02(5)}N_{1.98(5)}$

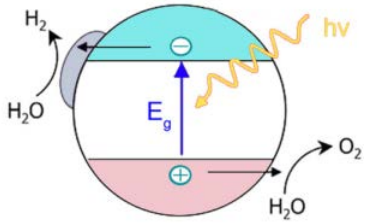

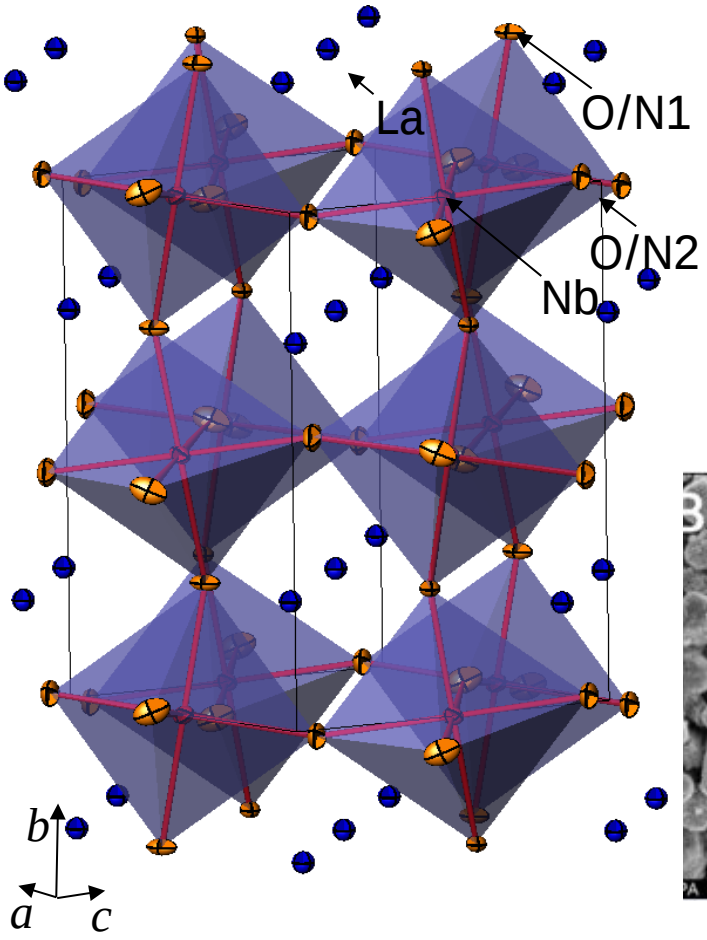

$$LaNbO_{4(s)} + 2NH_{3(g)} = LaNbON_{2(s)} + 3H_2O_{(g)}$$

- Bandgap 1.7 eV
- Hydrogen evolution rate: 12.7 µmol*g^{-1}*h^{-1}*m^{-2}

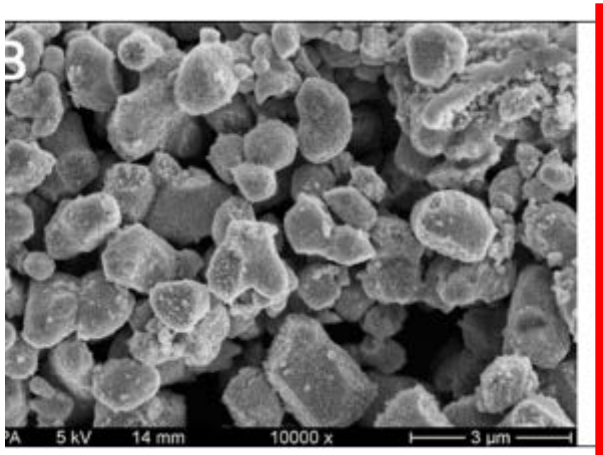

$LaNbON_2$
(without flux)

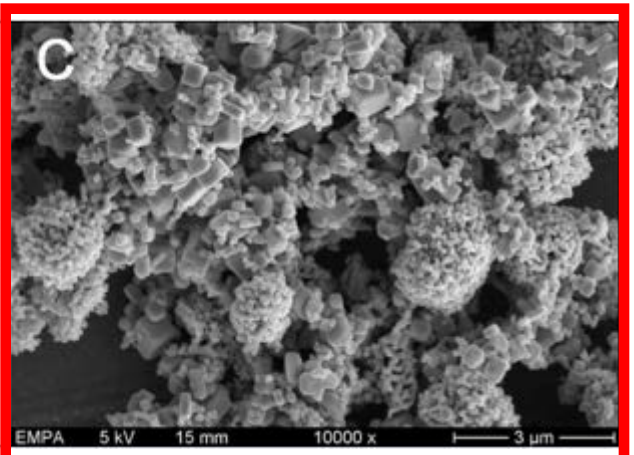

$LaNbON_2$
(flux assisted)

Logvinovich, D., Ebbinghaus, S. G., Reller, A. , Marozau, I., Ferri, D. and Weidenkaff, A. , Z. Anorg. Allg.Chem., 636 (2010)905-912.

EMPA
Materials Science & Technology

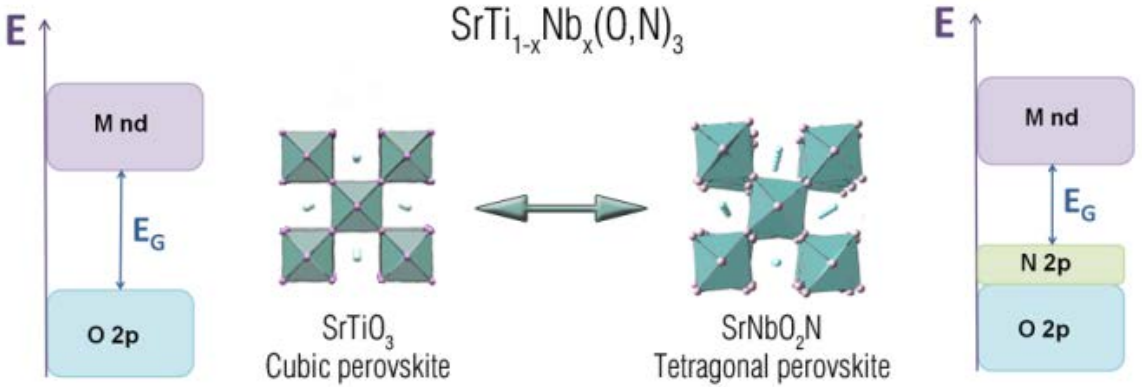

$SrTi_{0.95}Nb_{0.05}O_{2.94}N_{0.06}$

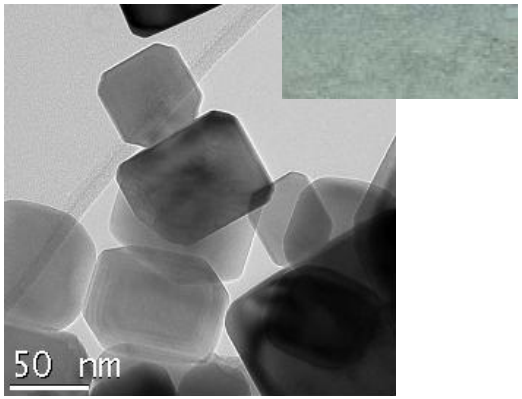

$SrTi_{0.50}Nb_{0.50}O_{2.55}N_{0.45}$

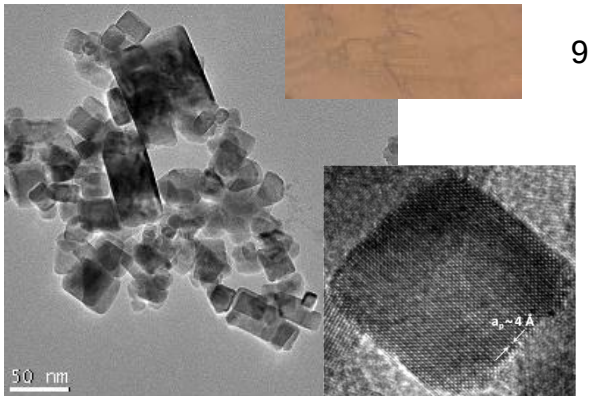

$SrTi_{0.05}Nb_{0.95}O_{2.11}N_{0.89}$

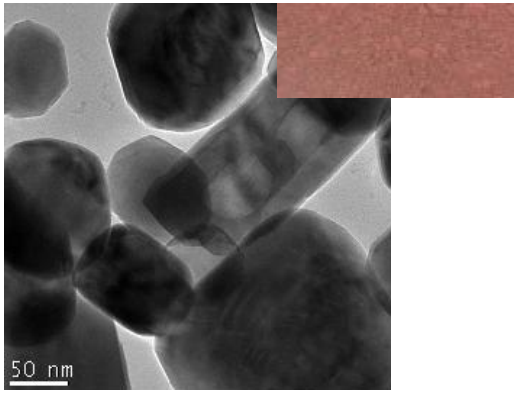

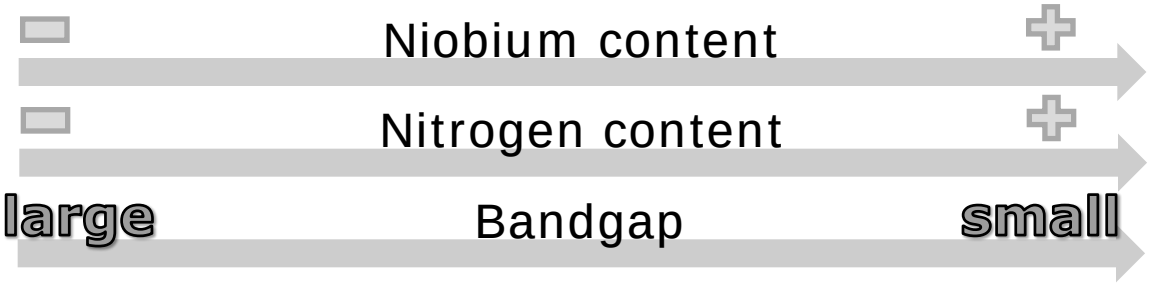

A. Maegli, S. Yoon, et al. *J.Solid State Chemistry*, **184** (2011) 929-936.

EMPA
Materials Science & Technology

Water photo-electrolysis on perovskite-type oxynitride thin films: surface states and band edge treatment

Reaction for $Sr_2Nb_2O_7$:

$$Sr_2Nb_2O_7 + 2\ NH_3 \leftrightarrow 2\ SrNbO_2N + 3\ H_2O$$

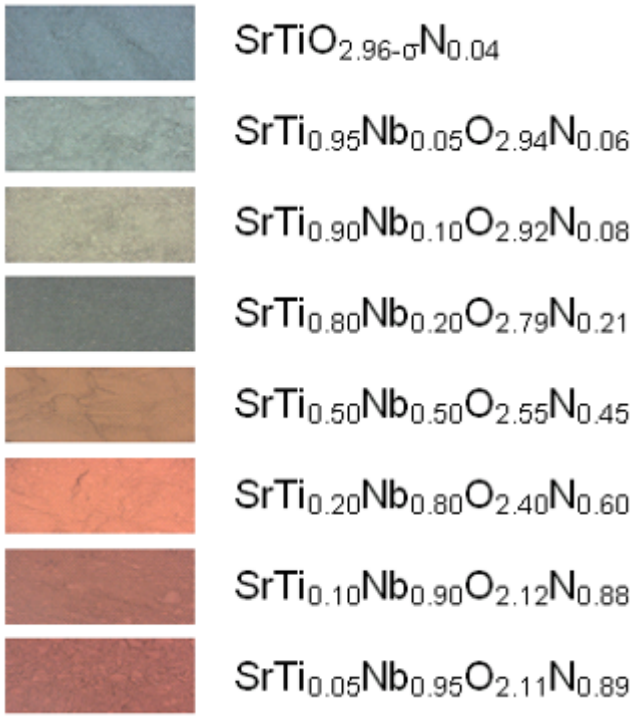

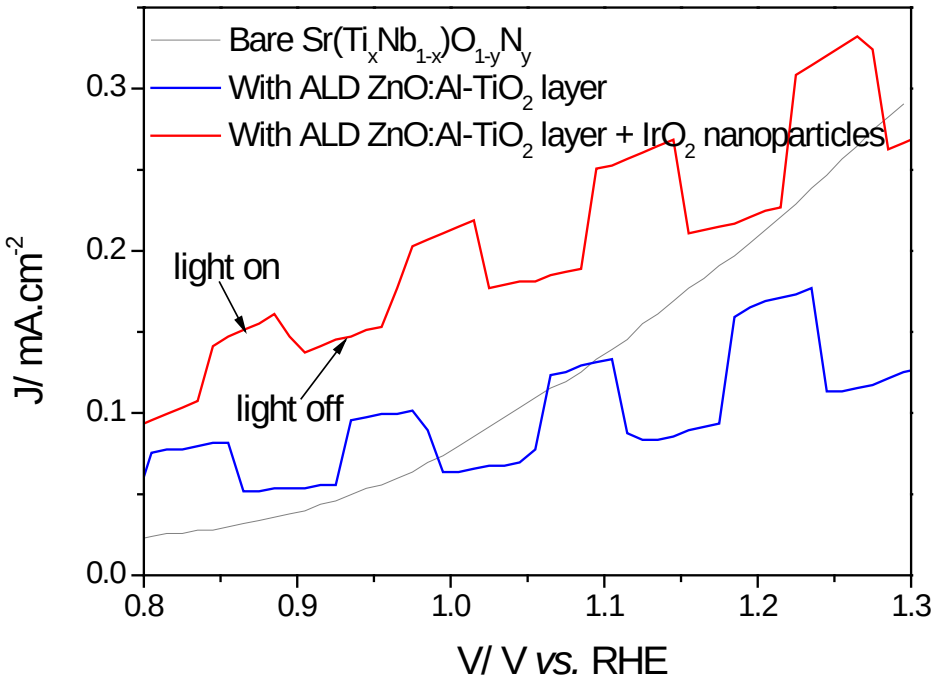

Leroy, C., M., Maegli, et al *Chem. Commun.* , Advance Article **48**, (2012) 820–822

EMPA
Materials Science & Technology

Watersplitting reaction with oxynitride perovskites

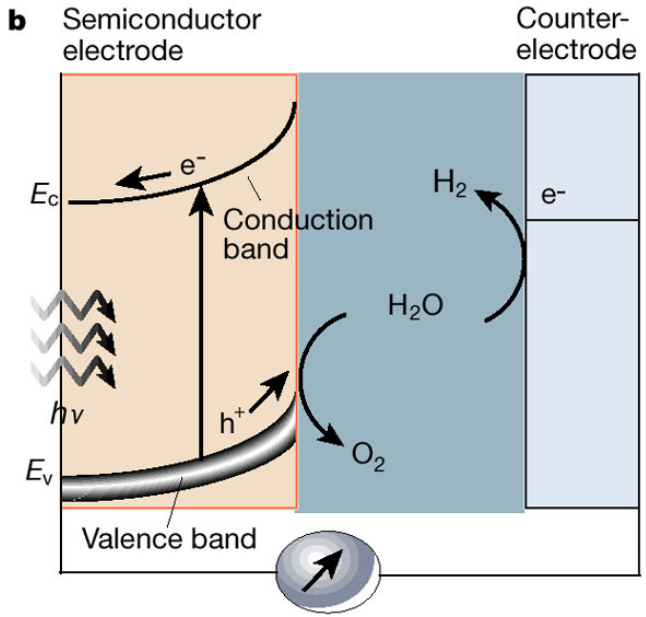

Grätzel, Nature (2001)

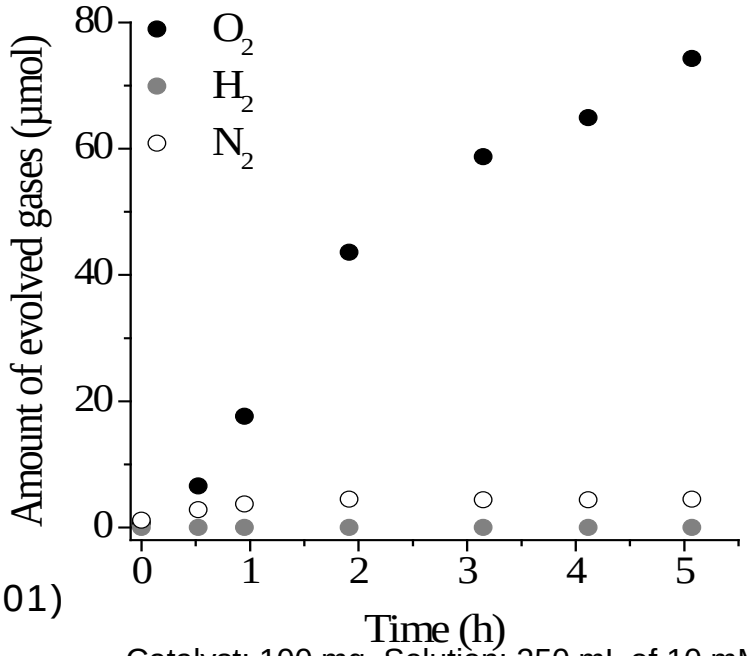

Catalyst: 100 mg, Solution: 250 mL of 10 mM $AgNO_3$ aq containing 200 mg of La_2O_3, Light source: a 150 W halogen lamp.

Test reaction for O_2 evolution

CB: $Ag^+ + e^- \rightarrow Ag$

VB: $2\ H_2O + 4\ h^+ \rightarrow O_2 + 4\ H^+$

$La_2O_3 + 6\ H^+ \rightarrow 2\ La^{3+} + 3\ H_2O$

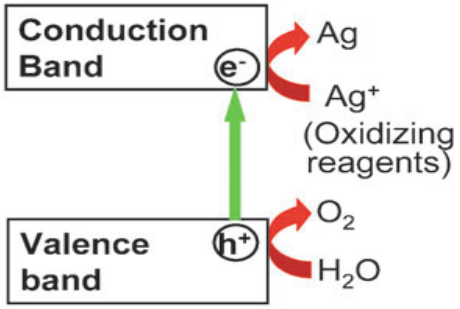

Kudo *et al*., Chem. Soc. Rev. (2009)

Leroy, C.et al., Chem. Commun. , Advance Article 48, (2012) 820–822

Why $LaTiO_2N$ for Water Splitting?

- Earth-abundant and inexpensive raw materials
- Band structure: Visible light absorption
- Band position: Straddle redox-potential of water splitting reaction
- High stability and regenerativity

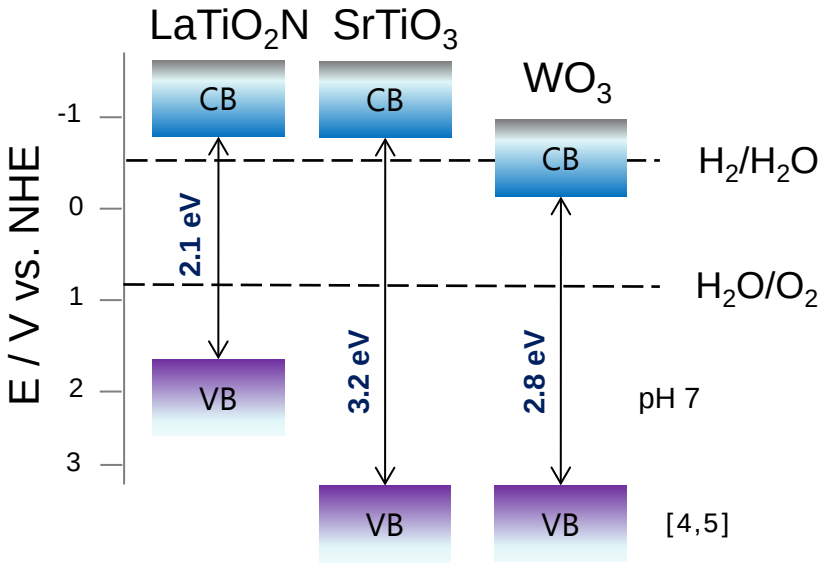

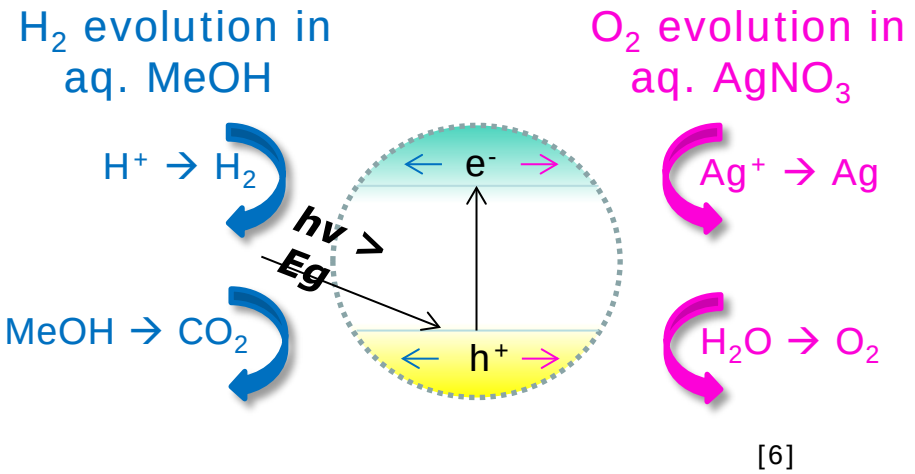

[4] C. Le Paven-Thivet *et al.*, J. Phys. Chem. C, 2009, 113. **[5]** A. Kudo and Y. Miseki, Chem. Soc. Rev., 2009, 38. **[6]** A. Kasahara *et al.*, J.Phys. Chem. A, 2002, 106. **[7]** N. Nishimura *et al.*, Thin Solid Films, 2010, 518. **[8]** C. M. Leroy *et al.*, Chem. Commun., 2012, 6.

$LaTiO_2N$: influence of ammonolysis on defect formations

- Band gap about 2.1 eV
- triclinic *I*-1(Clarke *et al.*, Logvinovich *et al.*) vs orthorombic Imma (Masatomo *et al.*)

Sample	O_2 µmol/h	Amount catalyst
TiO_2 (P-25)	7	0.1 g
$LaTiO_2N$	12	0.1 g
$LaTiO_2N:IrO_2$	41	0.2 g

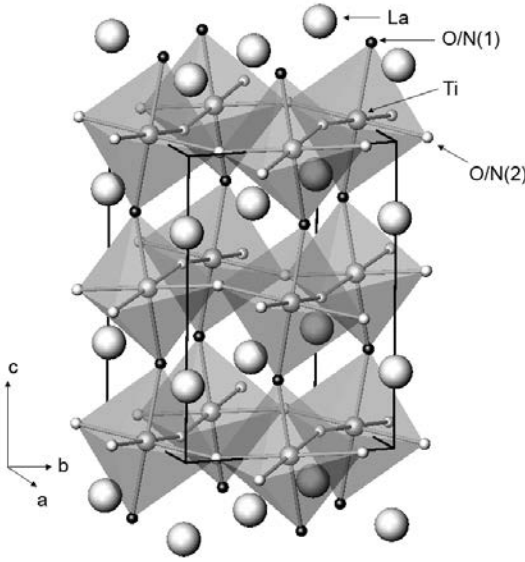

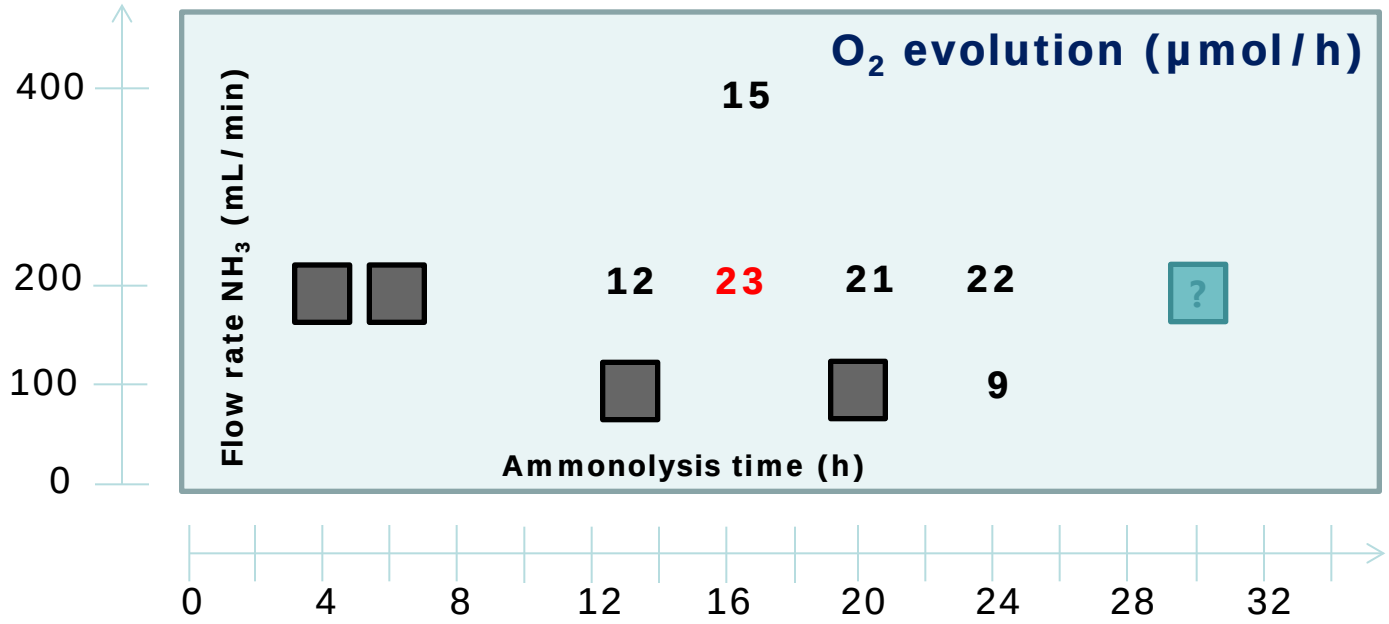

Catalyst, 100 mg

$AgNO_3$, 10 mM

La_2O_3, 200 mg

150 W halogen lamp

A. Maegli, T. Hisatomi, et al, Energy Proc. (2012) 61-66.

EMPA

Materials Science & Technology

Structural analysis: $La_{1-x}Ca_xTi(O,N)_3$

$LaTiO_2N$

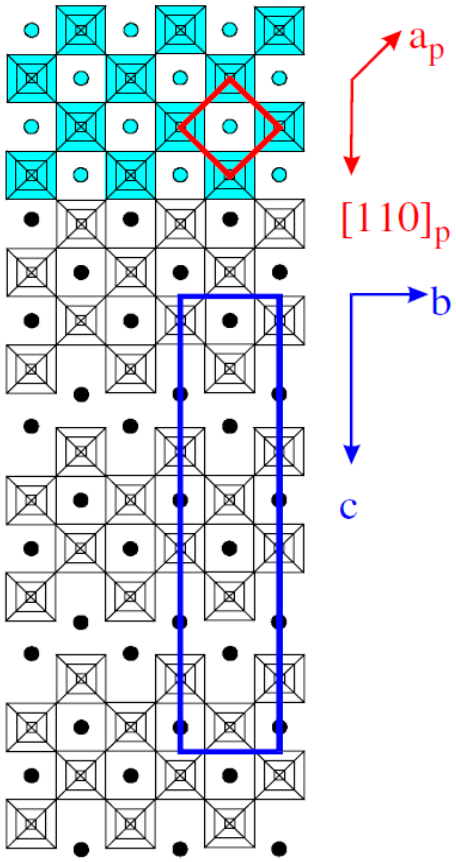

Thermal ammonolysis
(NH_3, > 800°C)

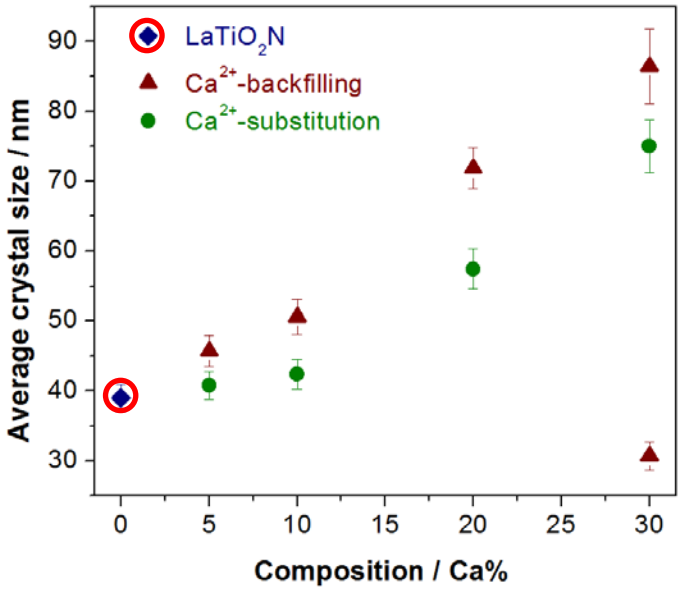

- Growth of crystallites with Ca

$LaTiO_{3.5}$ [9]

Precursor: Increasing amorphization with Ca^{2+}

Precursor: Facilitated ion-diffusion pathways
Facilitated topochemical condensation

S. G. Ebbinghaus *et al.*, Solid State Sci., 2008, 10.
R. Aguiar *et al.*, J. Mater. Chem., 2008, 18.

Photocatalytic oxygen evolution: Defects

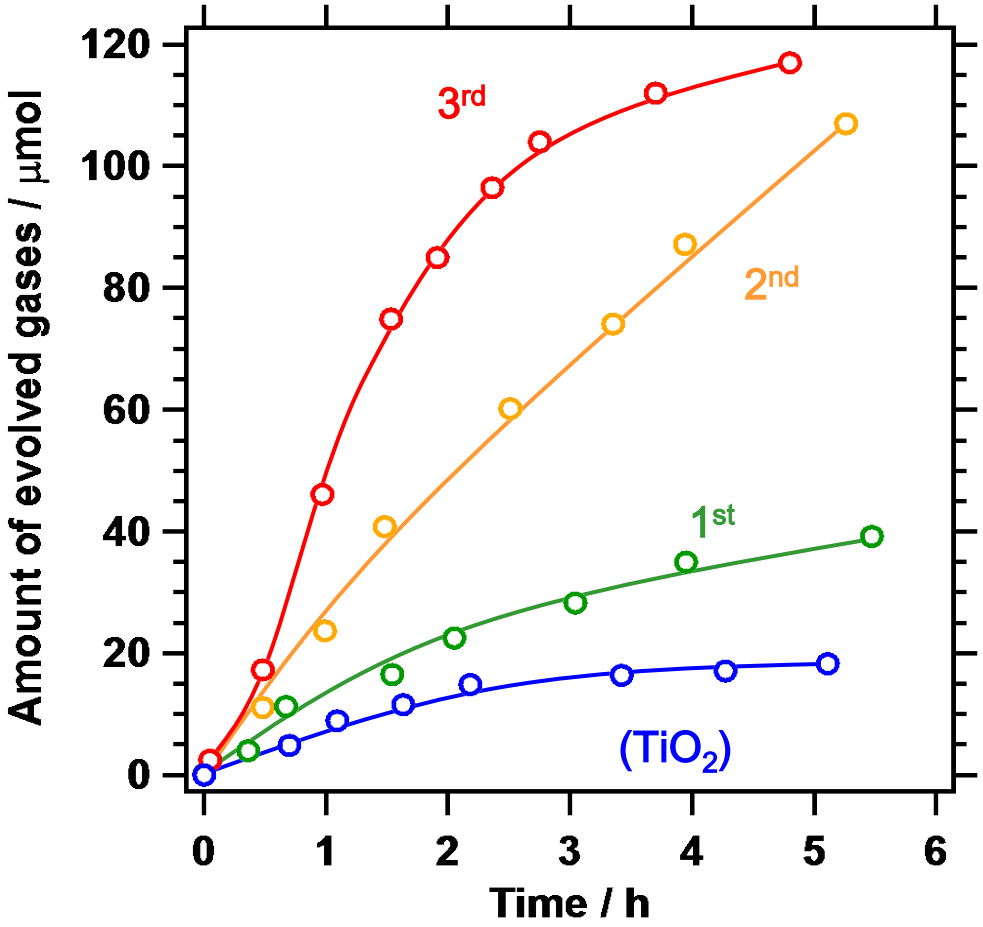

Increasing background absorption ➞ defects, d-d transitions Ti^{3+}

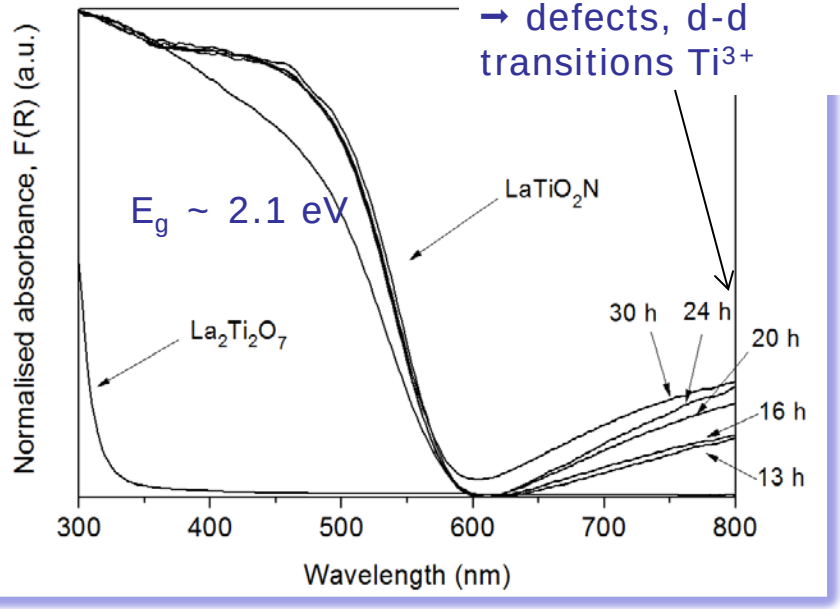

calculated from UV-vis diffuse reflectance

1st generation: $LaTiO_2N$
2nd generation: $(Ln,Ca)TiO_2N$
3rd generation: $(Ln,Ca)_+TiO_2N$:
5% A site-backfilled

Maegli, A. E., Structural and Photocatalytic Properties of Perovskite-Type $(La,Ca)Ti(O,N)_3$ Prepared from A-site Deficient Precursors, *J. Mater. Chem.* **22** (2012) 17906-17913.

EMPA
Materials Science & Technology

X-Ray Diffraction: Resulting $La_{1-x}Ca_xTi(O,N)_3$

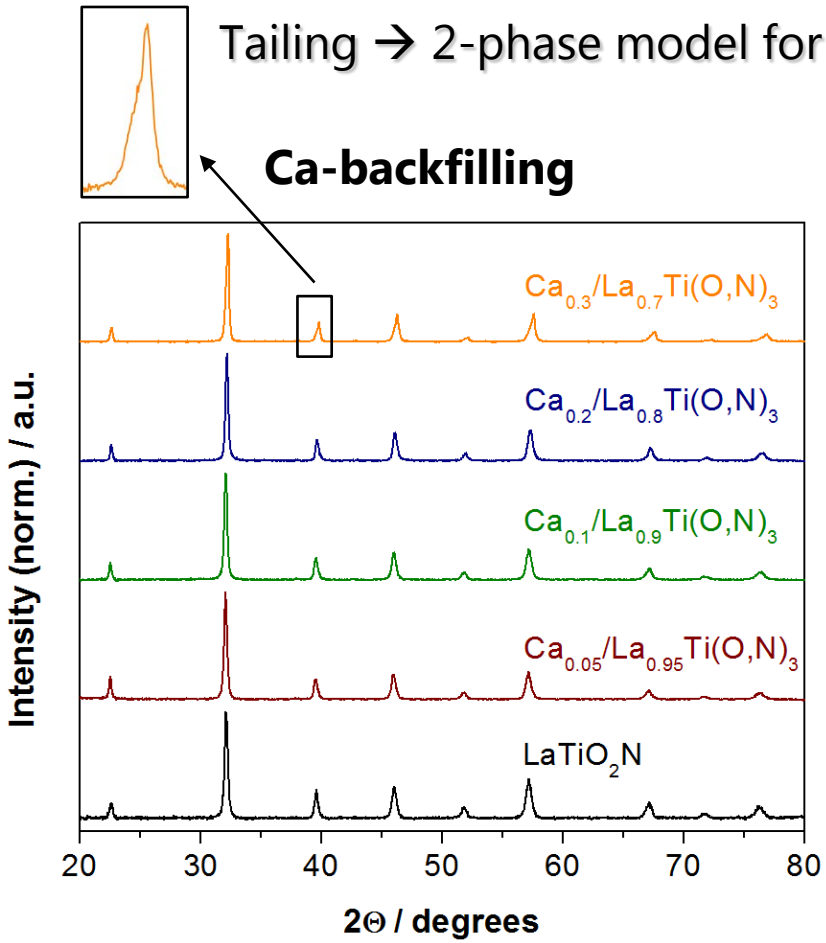

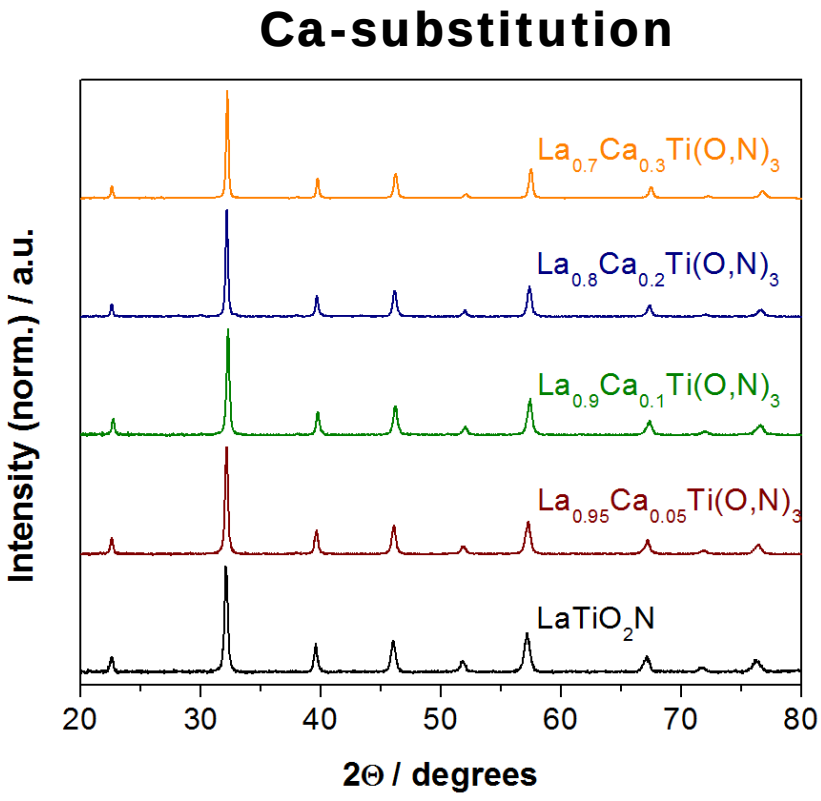

EMPA

Materials Science & Technology

From powder to the photoanode

Powder: $LaTiO_2N$ (reference)

↓

Electrophoretic deposition on conductive substrate (FTO)

↓

Necking with 0.1M ethanolic $TiCl_4$

↓

Calcination: 370 °C, 100 mL / min NH_3, 30 min

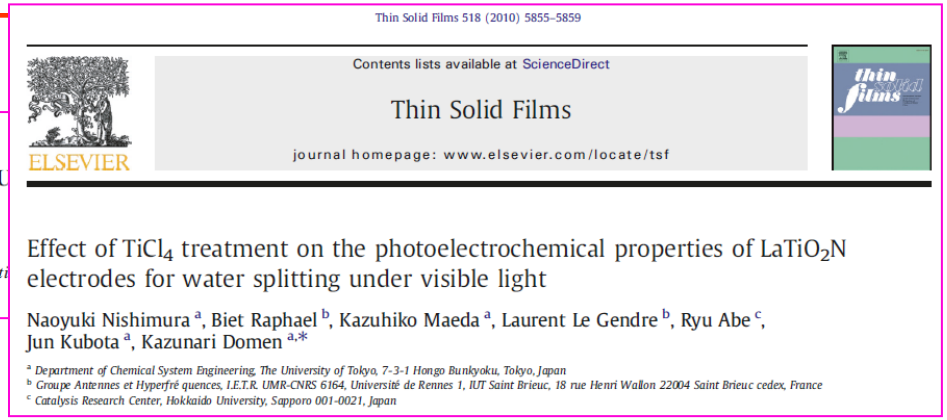

Thin Solid Films 518 (2010) 5855–5859

Contents lists available at ScienceDirect

Thin Solid Films

journal homepage: www.elsevier.com/locate/tsf

ELSEVIER

Effect of $TiCl_4$ treatment on the photoelectrochemical properties of $LaTiO_2N$ electrodes for water splitting under visible light

Naoyuki Nishimura [a], Biet Raphael [b], Kazuhiko Maeda [a], Laurent Le Gendre [b], Ryu Abe [c], Jun Kubota [a], Kazunari Domen [a,*]

[a] Department of Chemical System Engineering, The University of Tokyo, 7-3-1 Hongo Bunkyoku, Tokyo, Japan
[b] Groupe Antennes et Hyperfré quences, I.E.T.R. UMR-CNRS 6164, Université de Rennes 1, IUT Saint Brieuc, 18 rue Henri Wallon 22004 Saint Brieuc cedex, France
[c] Catalysis Research Center, Hokkaido University, Sapporo 001-0021, Japan

Facilitate e^- transport within porous electrode through TiO_{2-x} bridges between particles

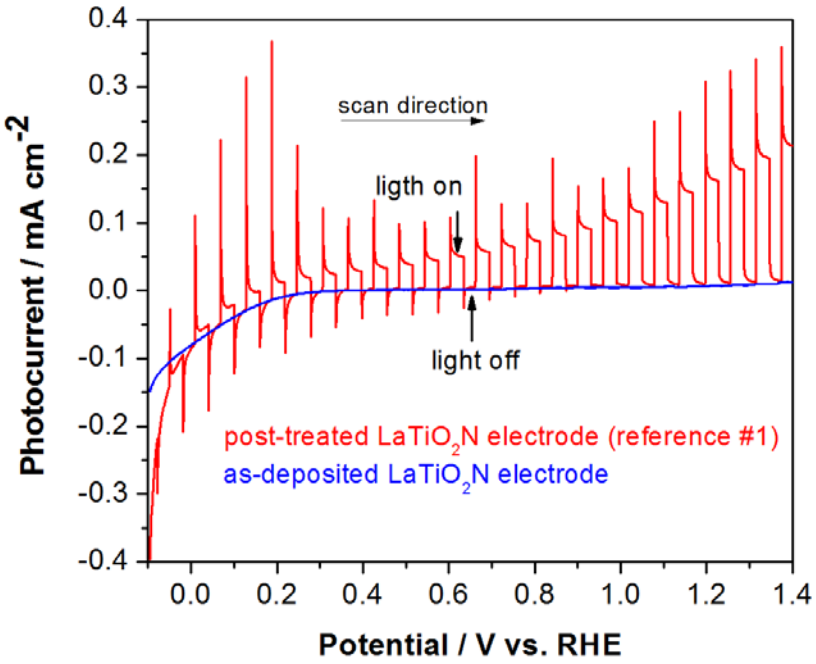

- Irradiation: Chopped AM 1.5
- Scan rate: 1 mV / s
- Electrolyte: 0.1M Na_2SO_4

Electrode Preparation by Electrophoretic deposition (EPD)

Conductive substrates: Fluorine-doped tin oxide (FTO)

Oxynitride powder, *e.g.* $LaTiO_2N$, modified $LaTiO_2N$, …

Suspension of powder in acteone-iodine solution
→ Adsorption of H^+ onto the suspended particles
→ Application of an electric field forces the particles to move to the cathode

Deposition of powder on the substrate
→ Application of different voltage / time allows to adjust thickness
→ Fast evaporation of solution, *i.e.* no removal of binders necessary

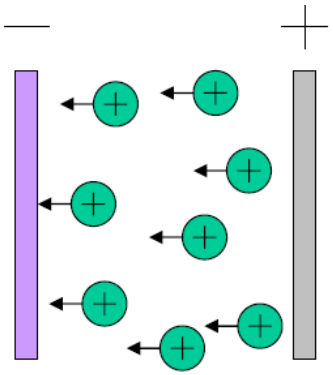

Cathodic EPD

1.25 cm

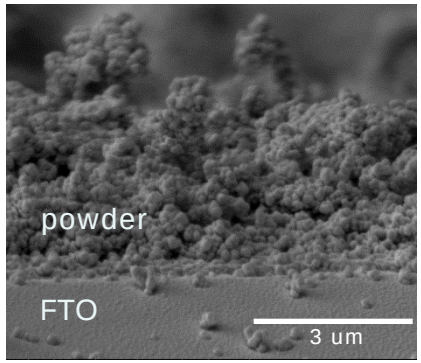

SEM cross-section of electrode

A. Mägli, C. Leroy, T. Hisatomi et al

Electrodes for the PEC water splitting cell

EPD of «LTON» onto FTO by cathodic EPD

→

heat-treatments under NH_3
→ Improvement of contact between oxynitride particles

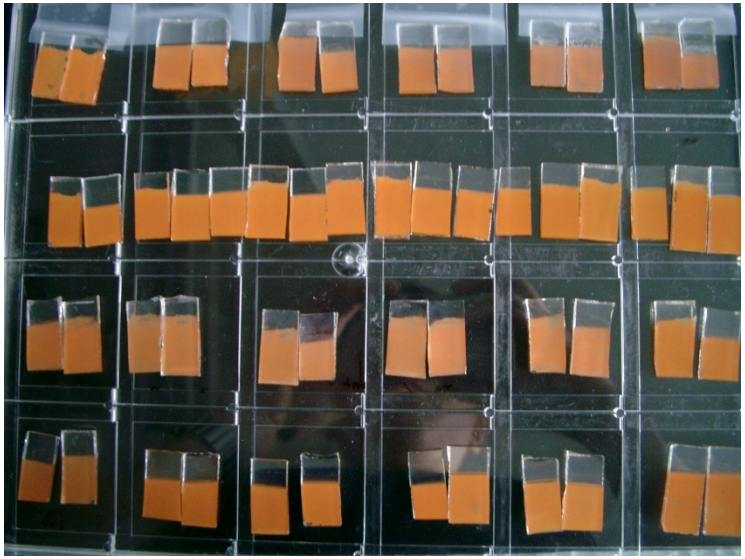

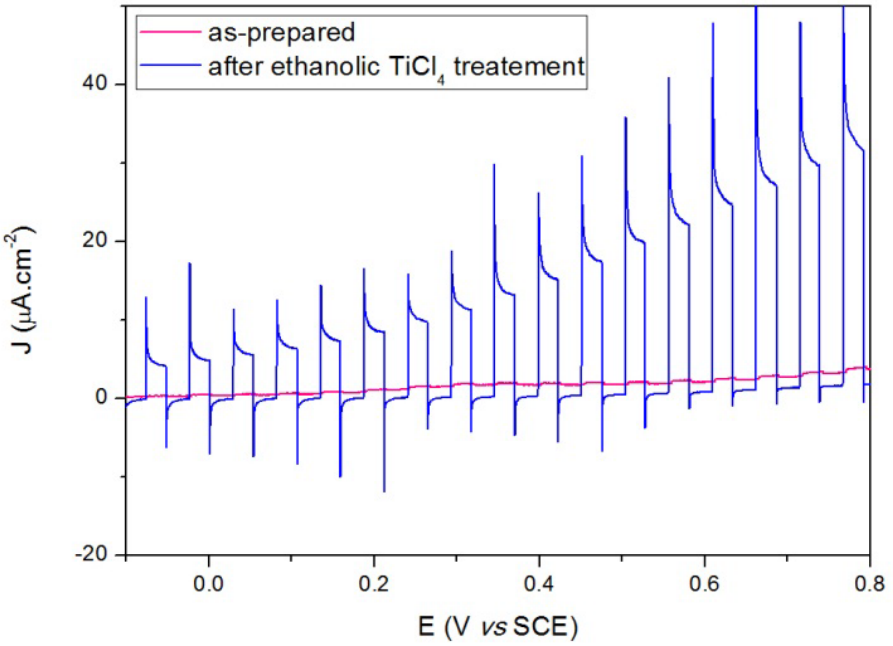

A. Mägli, T. Hisatomi, C.Leroy, M. Grätzel, A. Weidenkaff, et al, *Energy Proc.*, (2012) 61-66.

Comparison of electrodes I

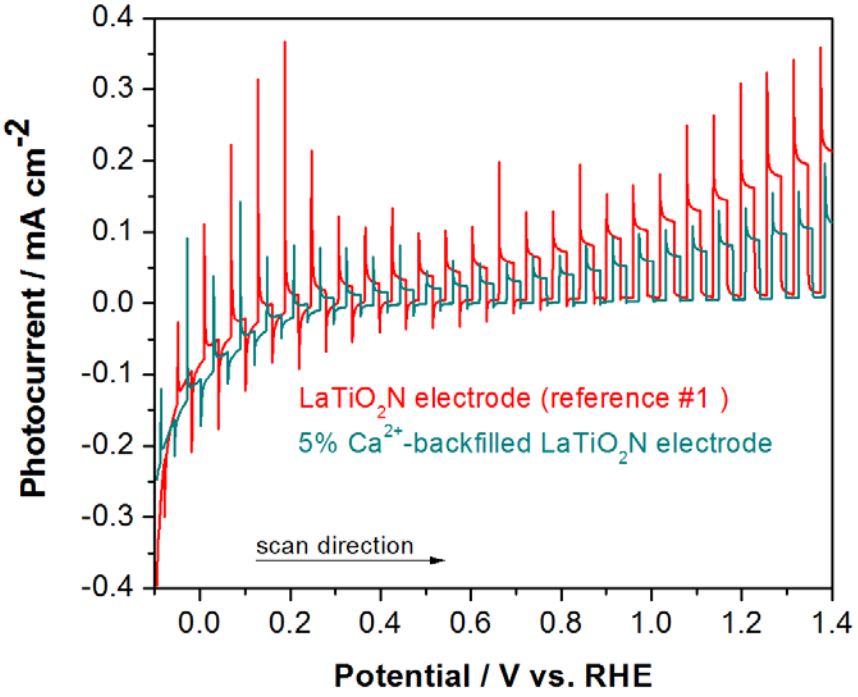

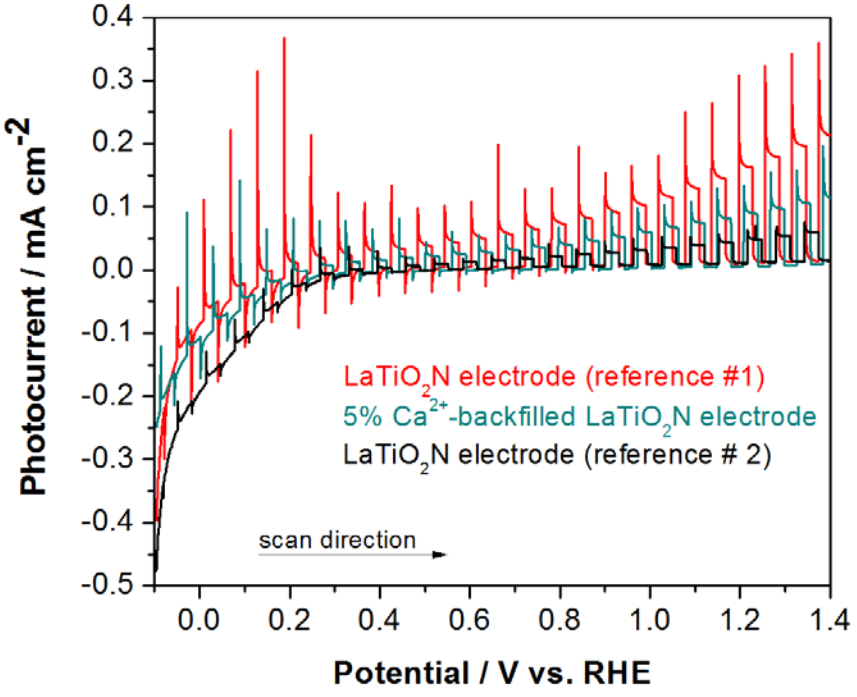

- Enhanced photocatalytic O_2 evolution of 5% Ca-backfilled $LaTiO_2N$ was not reflected in the potential – current measurements
- Reference #2 showed only ¼ of the photocurrent compared to reference #1
- What is making the difference?

Synopsis

O_2 evolution in aq. $AgNO_3$

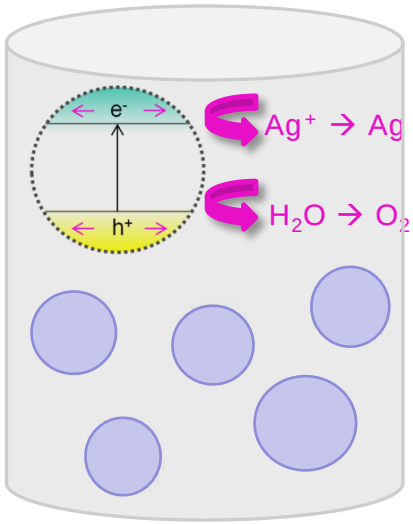

Efficiency of charge-carrier migration to particle surface

Bulk properties of powder

Photoanode in photoelectrochemical cell

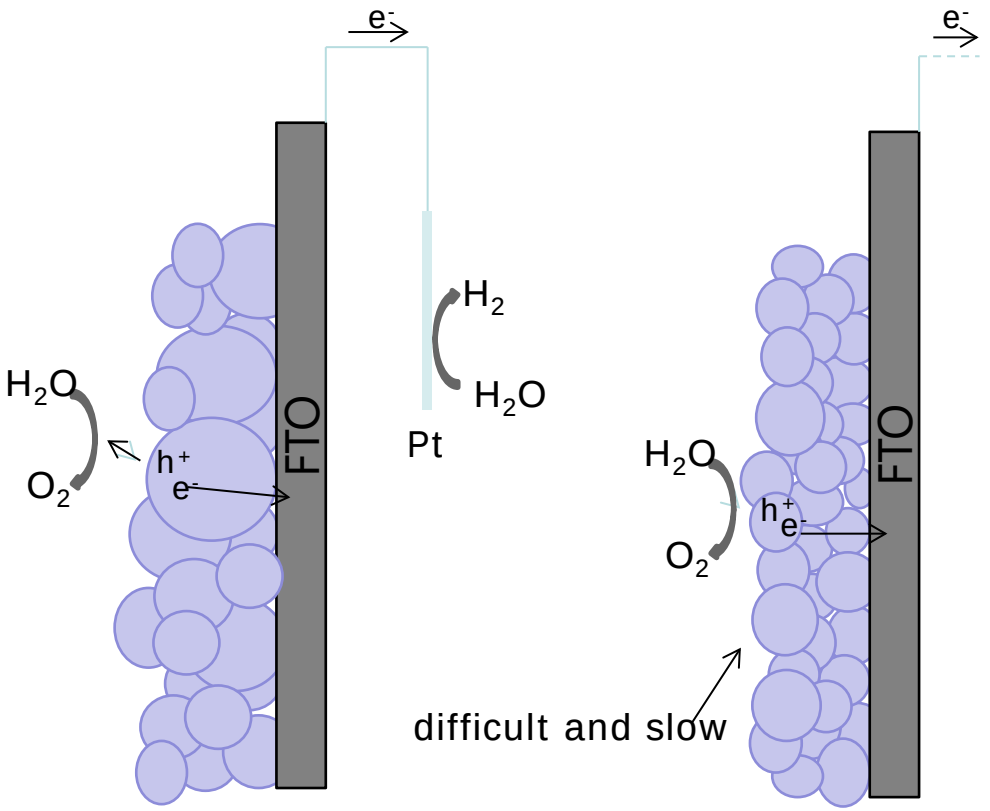

Efficiency of electron migration to FTO

Architecture of electrode

EMPA

Materials Science & Technology

Oxynitride perovskites are interesting materials for PEC

- ✓ efficient absorption of sunlight ✓
  perovskite-type oxynitrides band gaps are in the range of visible light
- ✓ chemical stability and durability ✓
  photo corrosion can be prevented by thin capping layers
- ✓ catalysis of water splitting reactions ✓
- ✓ separation and collection of photoexcited carriers ✓
  defects and traps in perovskite-type oxynitrides , low resistance

Photoelectrode	**Photocurrent (μA/cm^2) at +0.8 V *vs.* Ag/AgCl**
$LaTiO_2N$ (our lab)	193
$LaTiO_2N$ (Nishimura *et al.*, Thin Solid Films 518, 2010)	30
$LaTiO_2N$ (Le Paven-Thivet *et al.*, J. Phys. Chem. C 113, 2009)	40

Outline

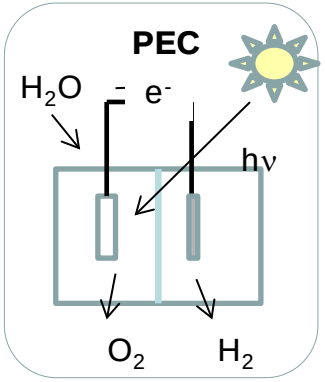

0.) Materials Design by 3D's, perovskites

1.) Solar H_2 by photoelectrochemistry

- ✓ Oxynitrides capture sunlight efficiently: appropriate E_g
- ✓ high catalytic activity: suitable surface of nanocrystallites

→ Gas evolution: 100 mg from 12 to >43 μmole/h

→ PEC: enhanced intergrain connectivity increases photocurrent

2.) High temperature Solar Thermoelectric converters

- ✓ chemical stability in air up to 1000K: Carnot ↗, energy density ↗
- ✓ large thermopower in good conductors: correlated electronic systems
- ✓ Phonon backscattering
- ✓ Thermoelectric oxides

  → from ZT<<0.1 to ZT > 0.4 to convert concentrated solar radiation.

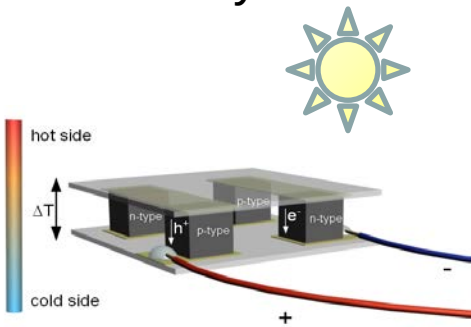

2.) High temperature Solar Thermoelectric converters

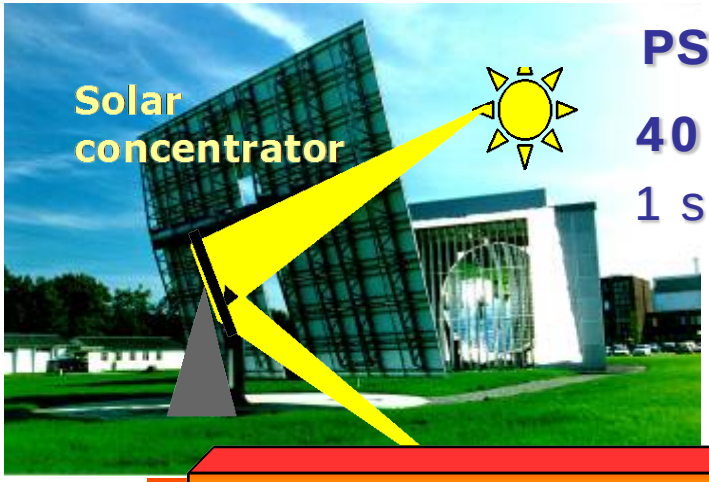

PSI

40 kW

1 sun =1 kW/m²

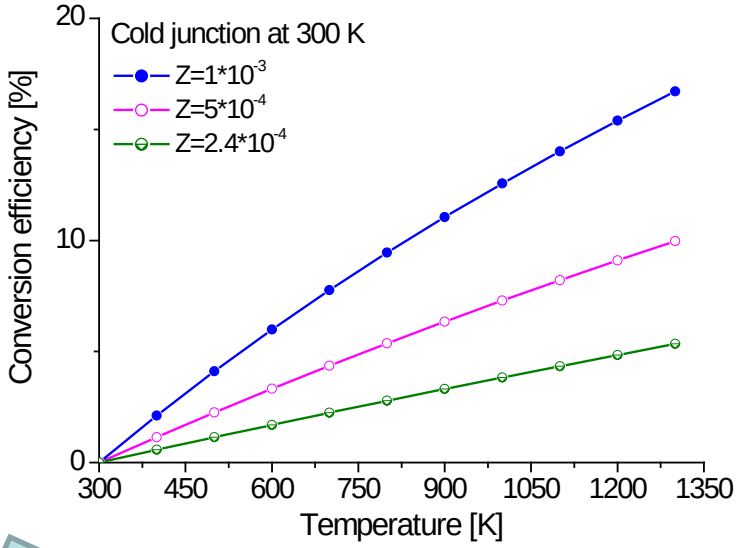

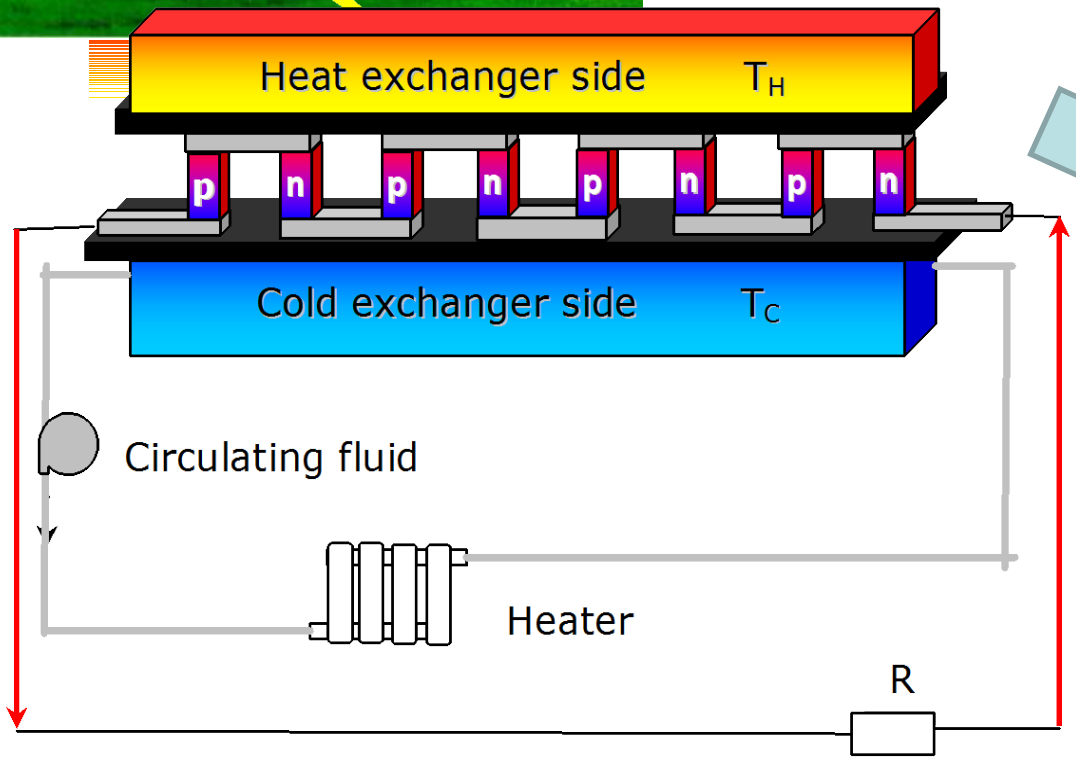

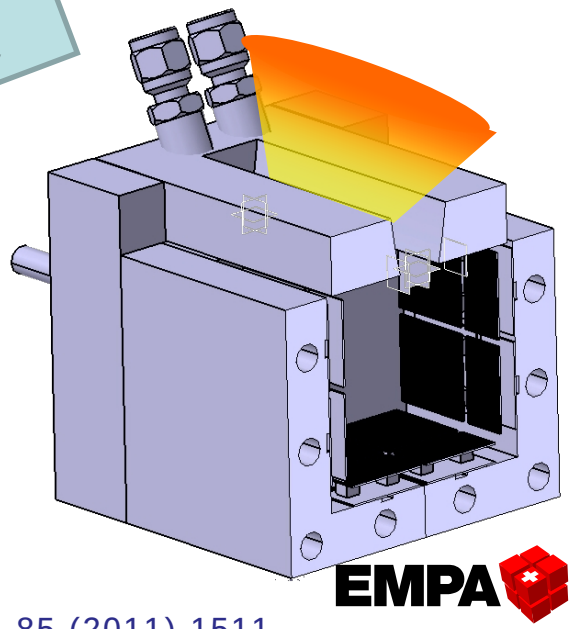

EMPA

Materials Science & Technology

C. Suter,Clemens, P. Tomeš, A. Weidenkaff, Anke, A. Steinfeld, *Solar Energy*, 85 (2011) 1511-1518.

Thermoelectric converters (heat → electricity)

thermoelectric *n*- and *p*-type thermocouples

$$S = -\frac{1}{e}\frac{\partial \mu}{\partial T}$$

$V = S \Delta T$

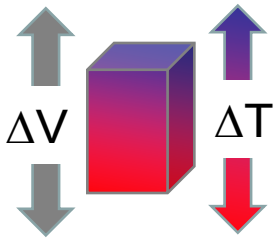

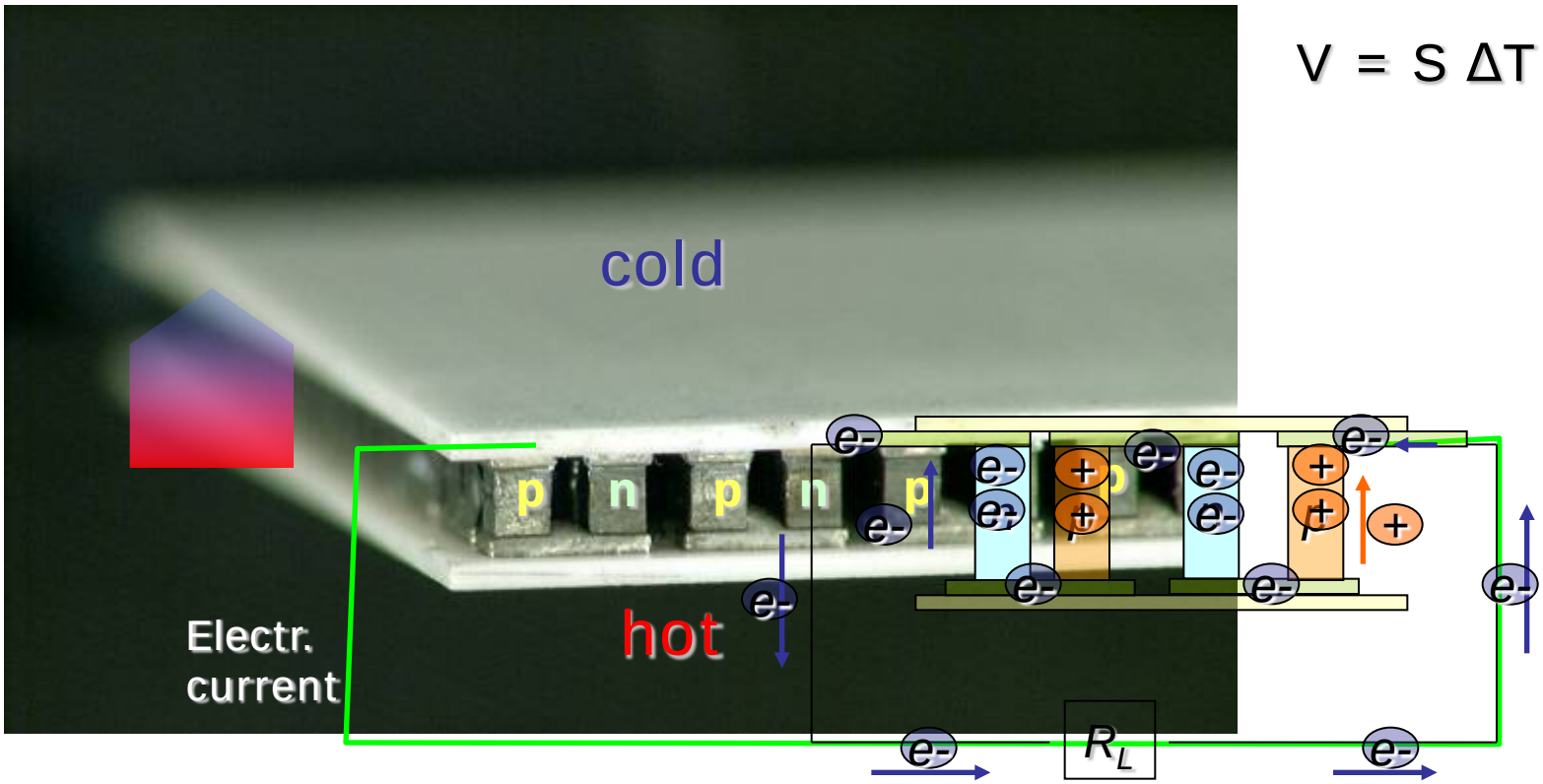

load R_a

EMPA

Materials Science & Technology

Materials requirements for HT thermoelectric converters

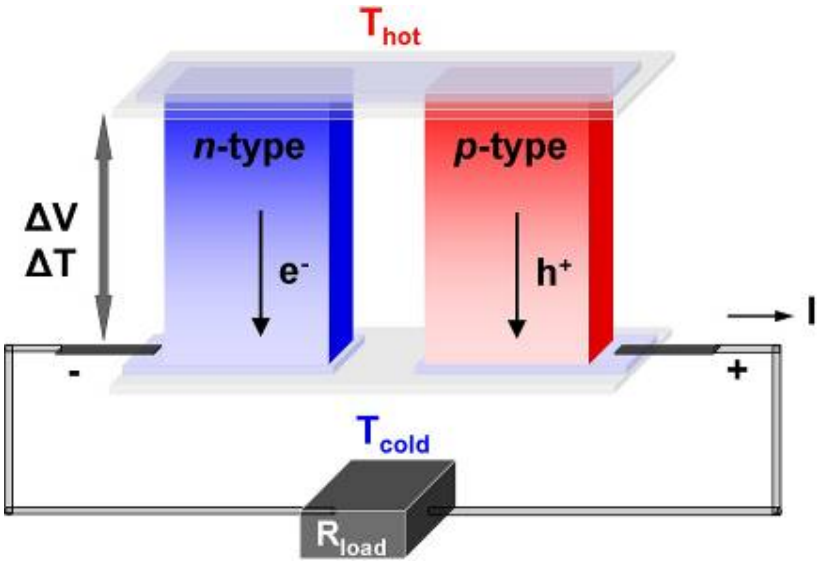

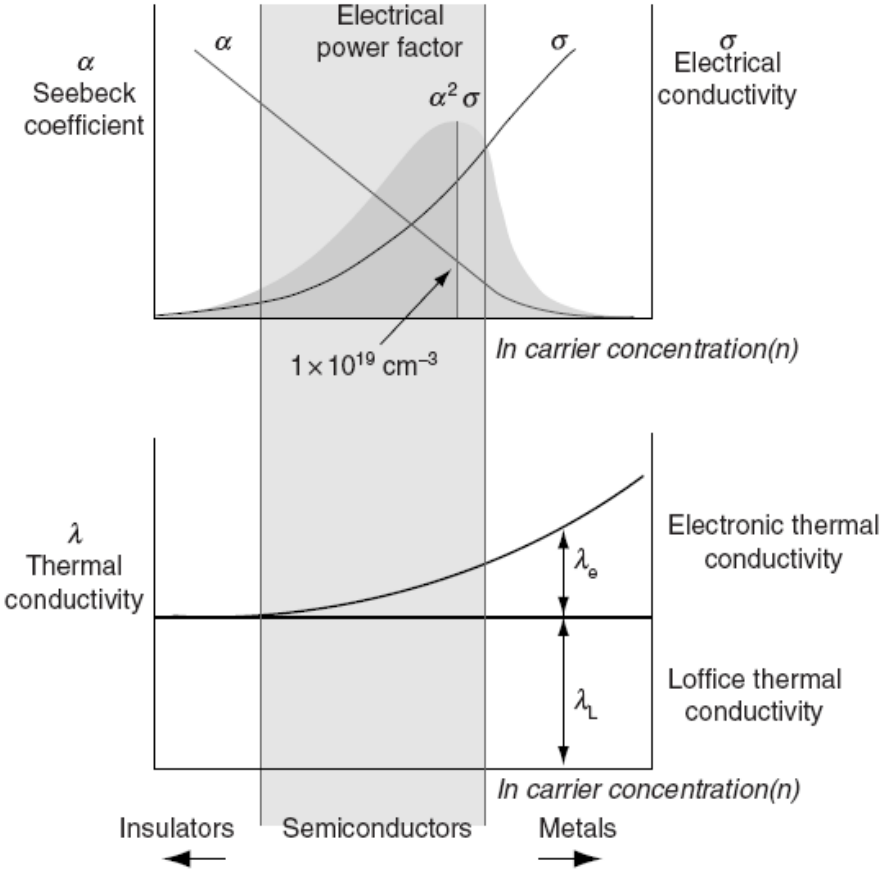

*D. M. Rowe, in Thermoelectric Handbook, 2006

Figure of merit

$$ZT = \frac{S^2\sigma}{\kappa}T$$

Seebeck coeff.

electr. cond.

heat cond.

- ✓ Stable @T_w in air
- ✓ *p*- und *n*-leg with similar S, σ, and κ
- ✓ High thermoelectric conversion efficiency and energy density

EMPA

Materials Science & Technology

Thermoelektrische Hochtemperatur-Materialien (HT)

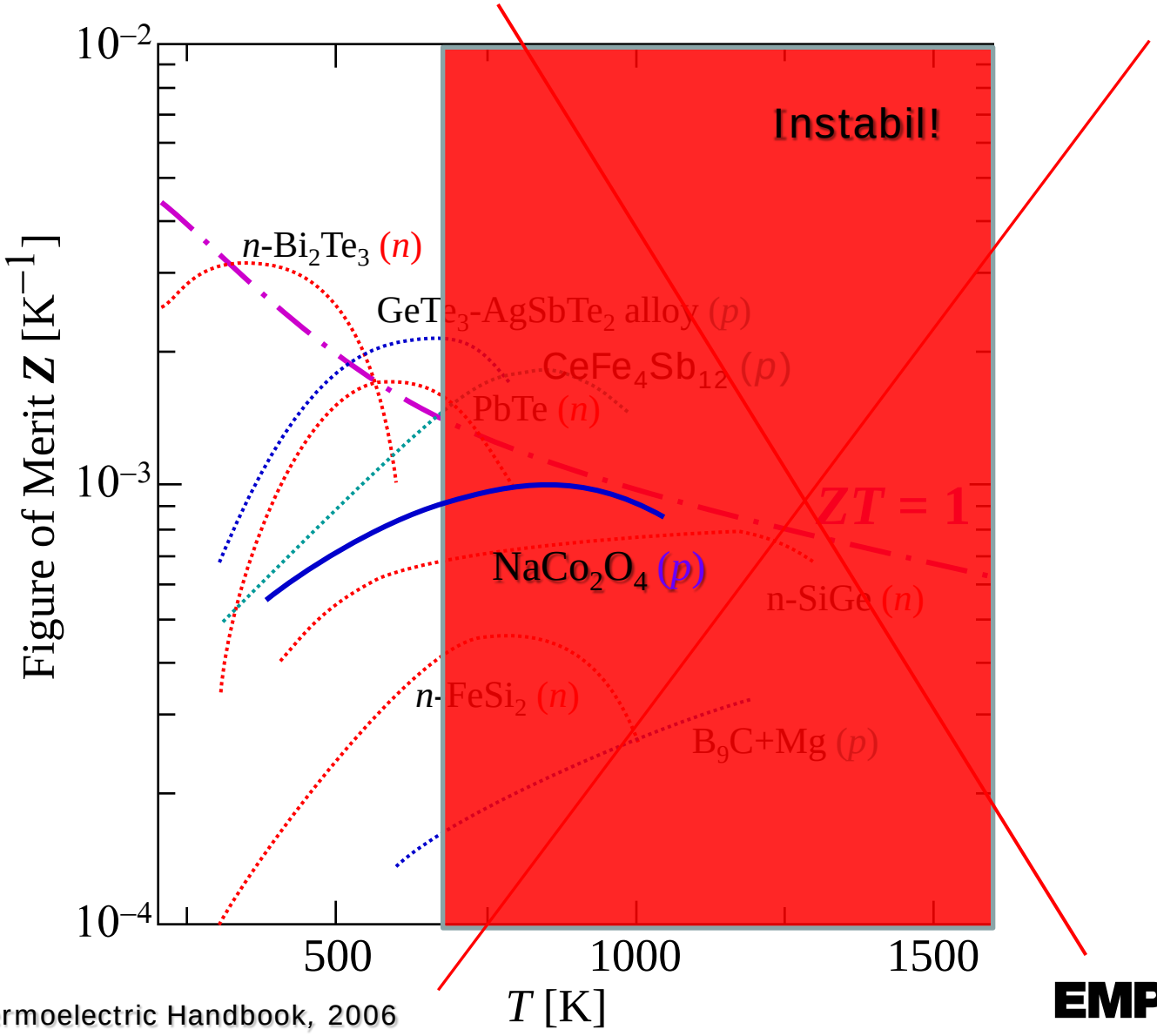

D. M. Rowe, in Thermoelectric Handbook, 2006
I. Terasaki et *al.*, PRB 56, R12685, 1997

Possible spin states and total degeneracy of ground-states of Co^{2+}, Co^{3+}, Co^{4+}

Ionic state	HS ($J_H > \Delta_{CF}$)		LS ($J_H < \Delta_{CF}$)		IS ($J_H \sim \Delta_{CF}$)	
	No distortion	Distortion ($\Delta_{JT} >> 0$)	No distortion	Distortion ($\Delta_{JT} >> 0$)	No distortion	Distortion ($\Delta_{JT} >> 0$)
Co^{2+}	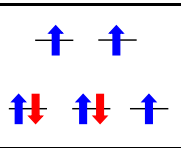	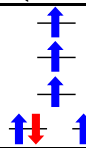	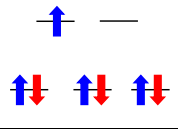	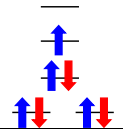	×	×
	$G_{spin} = 4$	$G_{spin} = 4$	$G_{spin} = 2$	$G_{spin} = 2$		
	$G_{orb} = 3$	$G_{orb} = 1$	$G_{orb} = 2$	$G_{orb} = 1$		
	Gtot = 12	**Gtot = 4**	**Gtot = 4**	**Gtot = 2**		
Co^{3+}	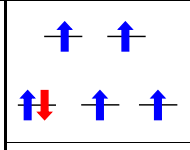	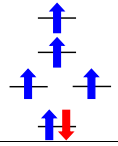	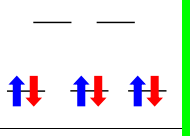	×	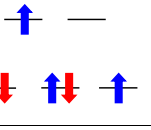	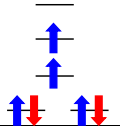
	$G_{spin} = 5$	$G_{spin} = 5$	$G_{spin} = 1$		$G_{spin} = 3$	$G_{spin} = 3$
	$G_{orb} = 3$	$G_{orb} = 1$	$G_{orb} = 1$		$G_{orb} = 6$	$G_{orb} = 1$
	Gtot = 15	**Gtot = 5**	**Gtot = 1**		**Gtot = 18**	**Gtot = 3**
Co^{4+}	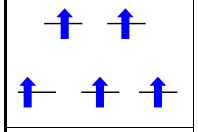	×	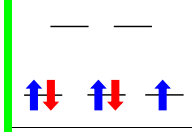	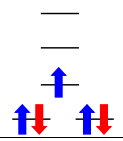	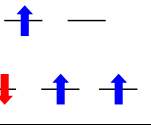	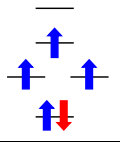
	$G_{spin} = 6$		$G_{spin} = 2$	$G_{spin} = 2$	$G_{spin} = 4$	$G_{spin} = 4$
	$G_{orb} = 1$		$G_{orb} = 3$	$G_{orb} = 1$	$G_{orb} = 6$	$G_{orb} = 1$
	Gtot = 6		**Gtot = 6**	**Gtot = 2**	**Gtot = 24**	**Gtot = 4**

Mobile charge carriers produce an entropy current and a charge current.

- strongly correlated 3d (or 4d) electrons
- hybridization of charge carriers energy
- spin of the electrons can also be a source of entropy

Spin-entropy term

Entropy : $k_B \ln 6$ -> thermopower of $k_B \ln 6/|e|$

$$S_{mag+orb} = -\frac{k_B}{e}\ln\left(\frac{G_{spin+mag}^{Co^{4+}}}{G_{spin+mag}^{Co^{3+}}}\right) = +273\mu VK^{-1}, S_{mag+spin} = -\frac{k_B}{e}\ln\left(\frac{G_{mag}^{Co^{4+}}}{G_{mag}^{Co^{3+}}}\right) = +154\mu VK^{-1}$$

Adapted from Jiri Hejtmanek, Prague and Ichiro Terasaki, Nagoya

EMPA
Materials Science & Technology

High temperature thermoelectric oxides

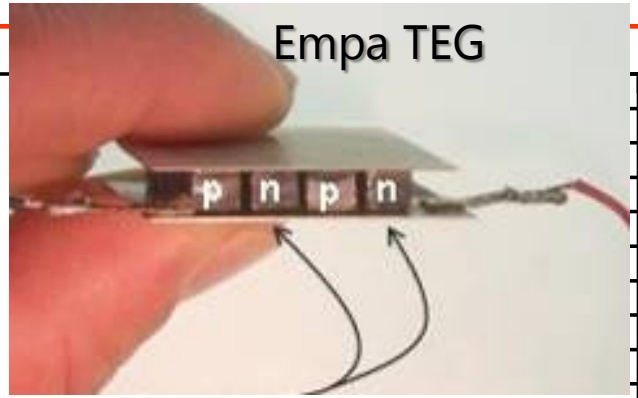

Data from (1) K. Fujita et *al.*, Jpn. J. Appl. Phys. 40, 4644 (2001), (2) M. Mikami et *al.*, J. Appl. Phys. 94, 5144 (2003), (3) M. Shikano et *al.*, Appl. Phys. Lett. 82, 1851 (2003), (4) G. Xu et *al.*, Appl. Phys. Lett. 80, 3760 (2002), **(5) R. Funahashi et *al.*, Appl. Phys. Lett. 81, 1459 (2002),** (6) R. Robert, et *al.*, Acta Mater. 55, 4965 (2007), (7) H. Muta et *al.*, J. Alloys Compd.350, 292 (2003) (Results obtained under argon atmosphere), (8) H. Ohta et *al.*, Nat. Mater. 6, 129 (2007), **(9) M. Ohtaki et *al.*, J. Appl. Phys. 79, 1816 (1996),** (10) L. Bocher et *al.*, Inorg. Chem. 47, 8077 (2008).

Thermoelectric properties of $EuTiO_{3-\delta}$ & $EuTi_{0.98}Nb_{0.02}O_{3-\delta}$

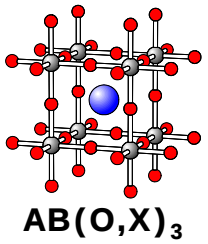

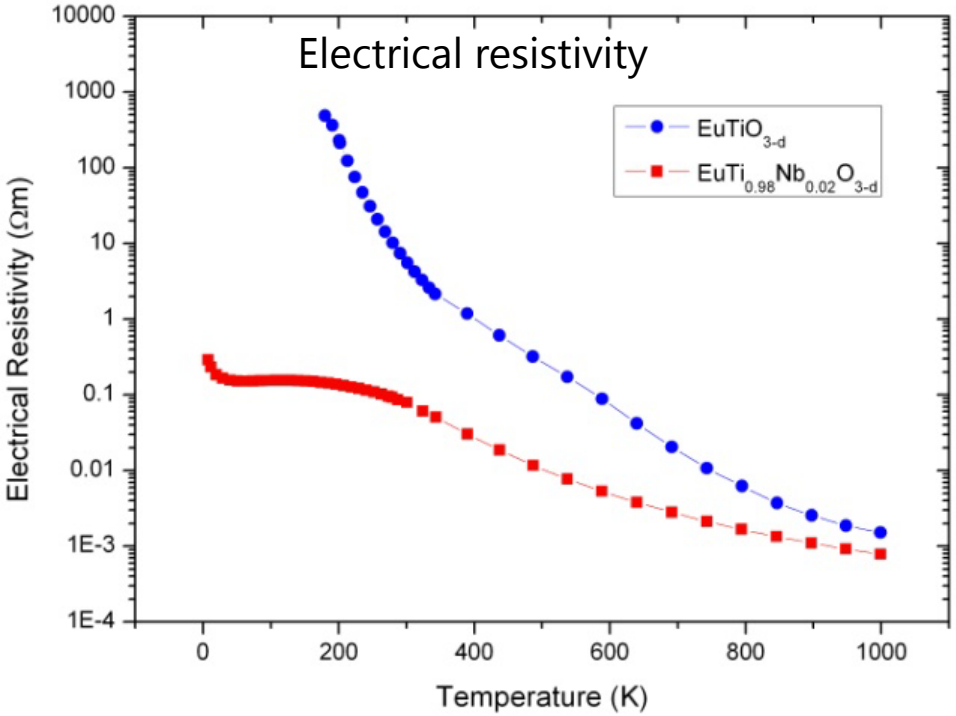

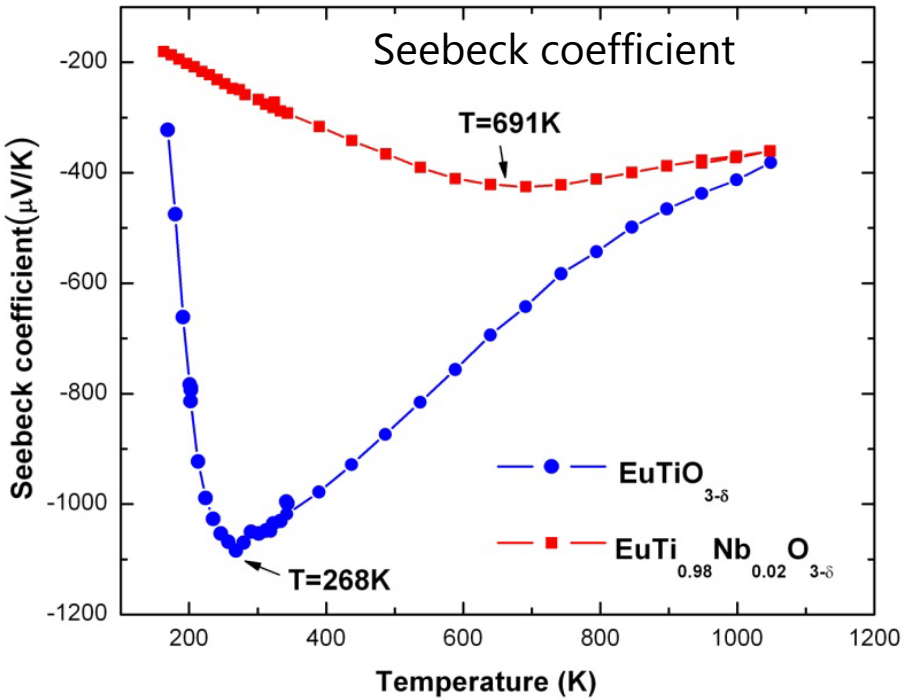

- Decrease of ρ by Nb 2% substitution: one order of magnitude at high T

- $EuTiO_3$ is one of the oxides with highest $|S|$ = 1081 μV/K at T = 268 K

L. Sagarna et al, *Appl. Phys. Lett.* **101**, (2012) 033908APL, 2012.

EMPA
Materials Science & Technology

Thermoelectric properties of $EuTiO_{3-d}$ & $EuTi_{0.98}Nb_{0.02}O_{3-d}$

Figure of Merit:

$$ZT = \frac{S^2\sigma}{\kappa} T$$

$EuTi_{0.98}Nb_{0.02}O_3$
ZT = 0.43 at T = 1040 K

$EuTiO_3$
ZT = 0.37 at T = 1090 K

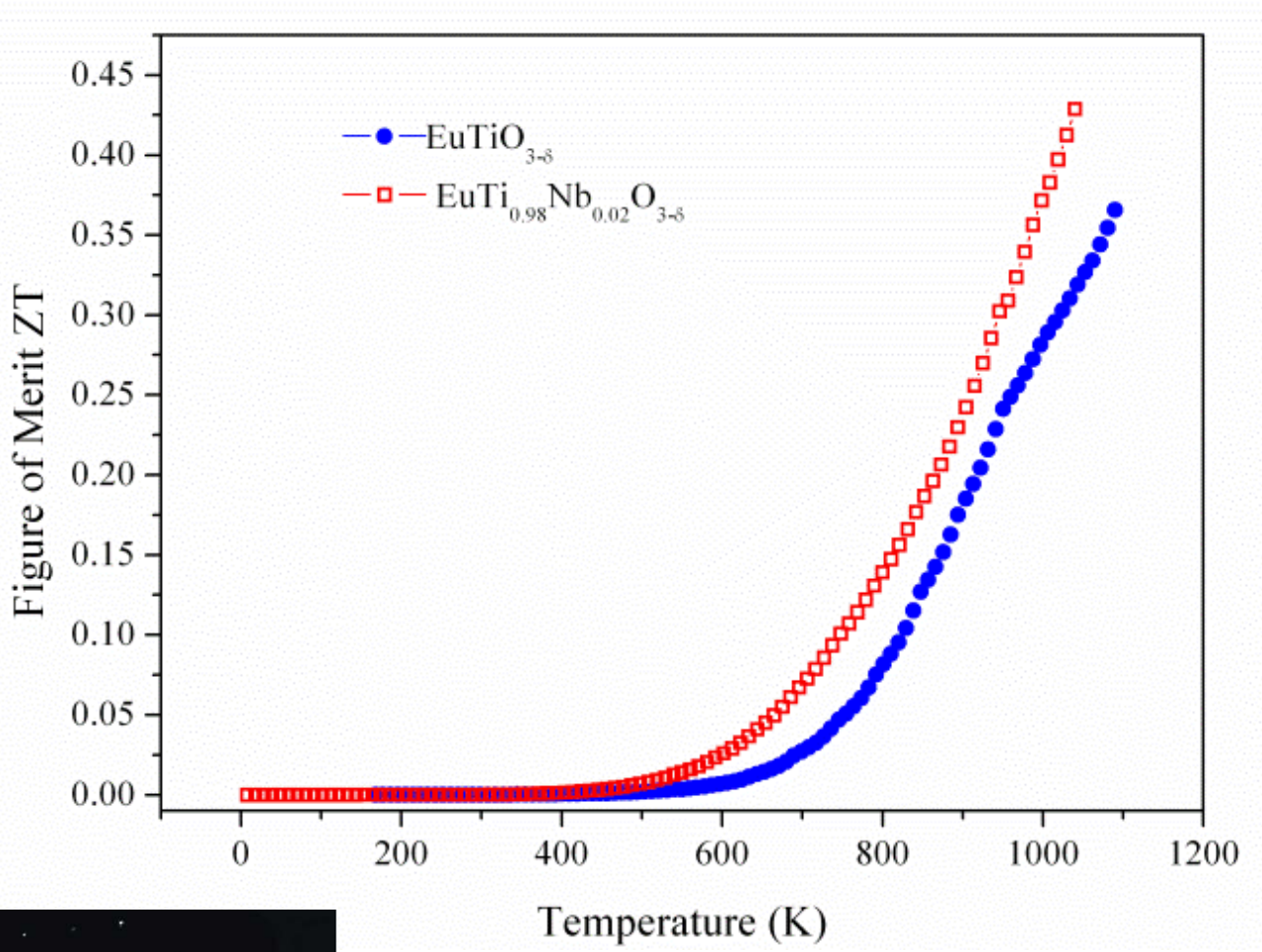

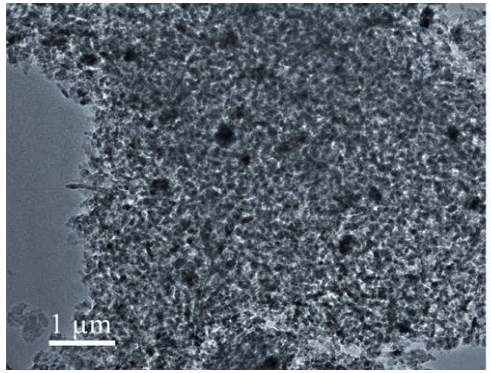

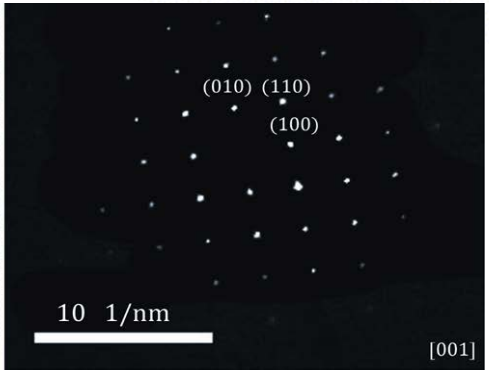

EMPA
Materials Science & Technology

Simulation of TE conversion: compatability factor

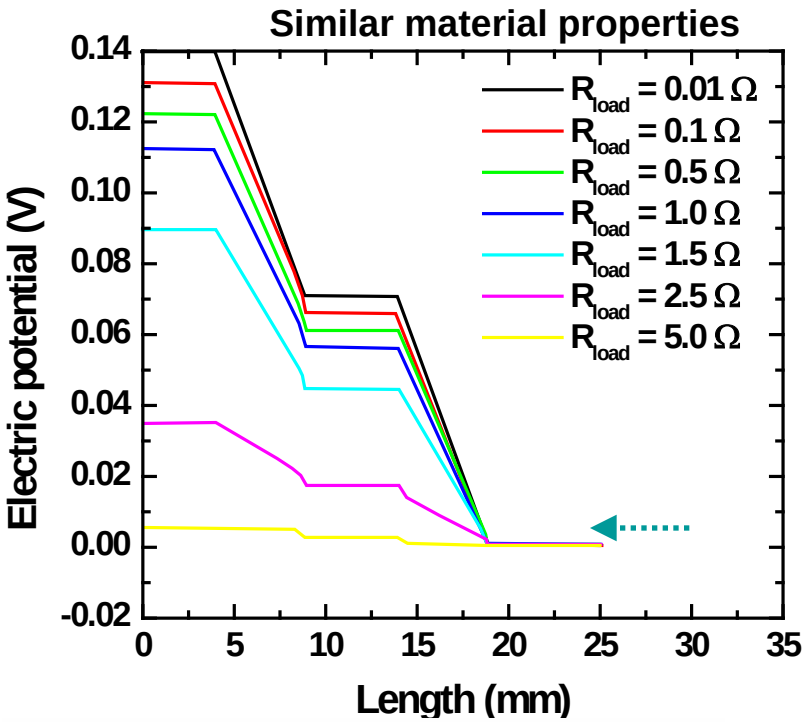

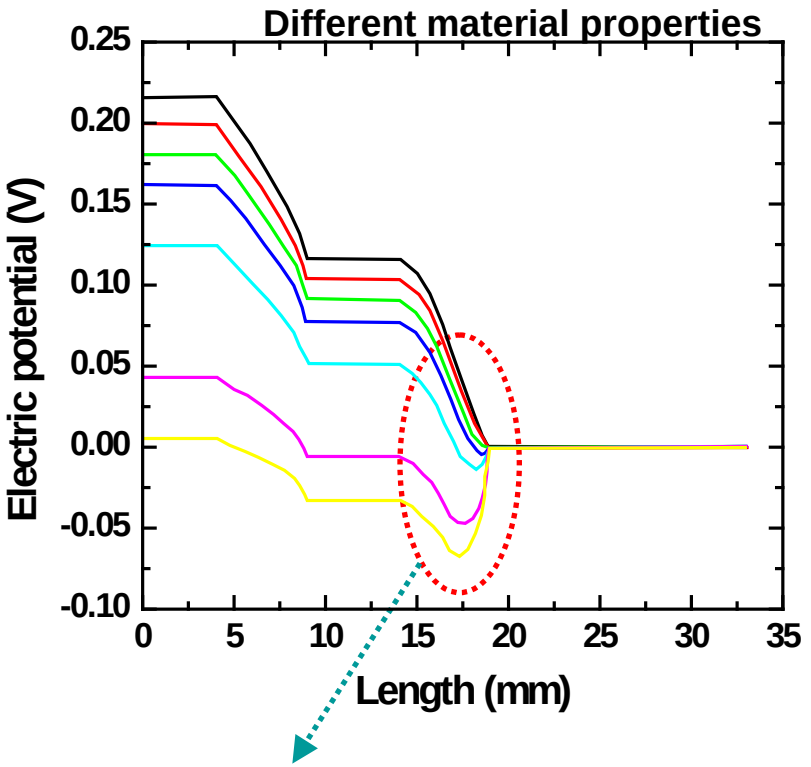

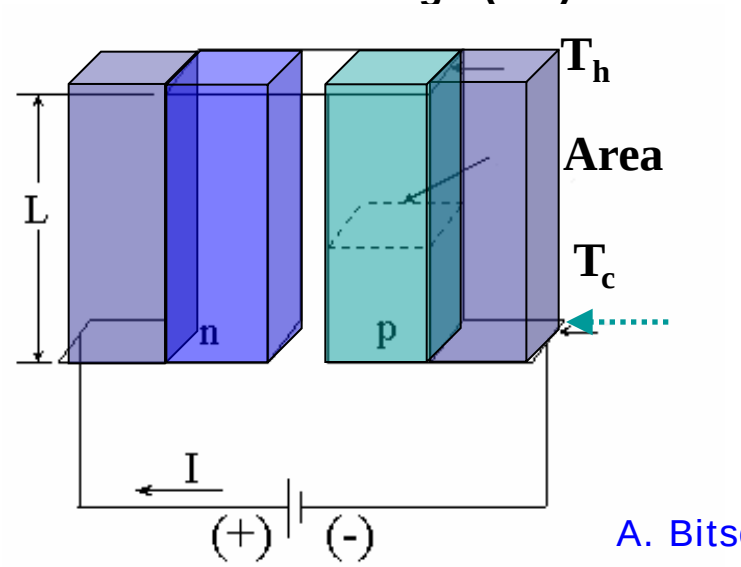

Voltage losses due to different resistance values of the *p*- and *n*-type legs.

A. Bitschi , P. Tomes- Comsol Multiphysics

The 34-leg TOM with ZT<< 0.1 ($La_{1.98}Sr_{0.02}CuO_4$) *p*-legs

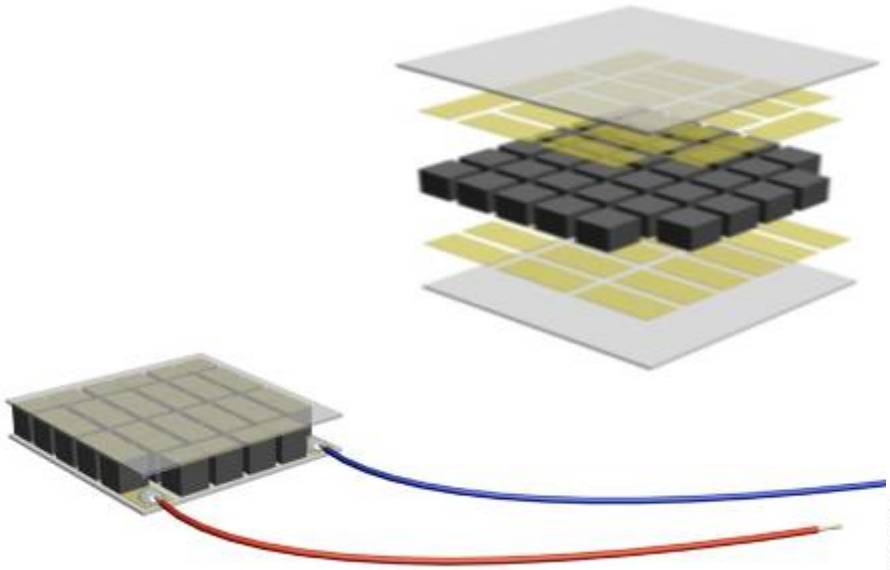

p-type: $La_{1.98}Sr_{0.02}CuO_4$ (ZT = 0.05)

n-type: $CaMn_{0.98}Nb_{0.02}O_3$ (ZT = 0.15)

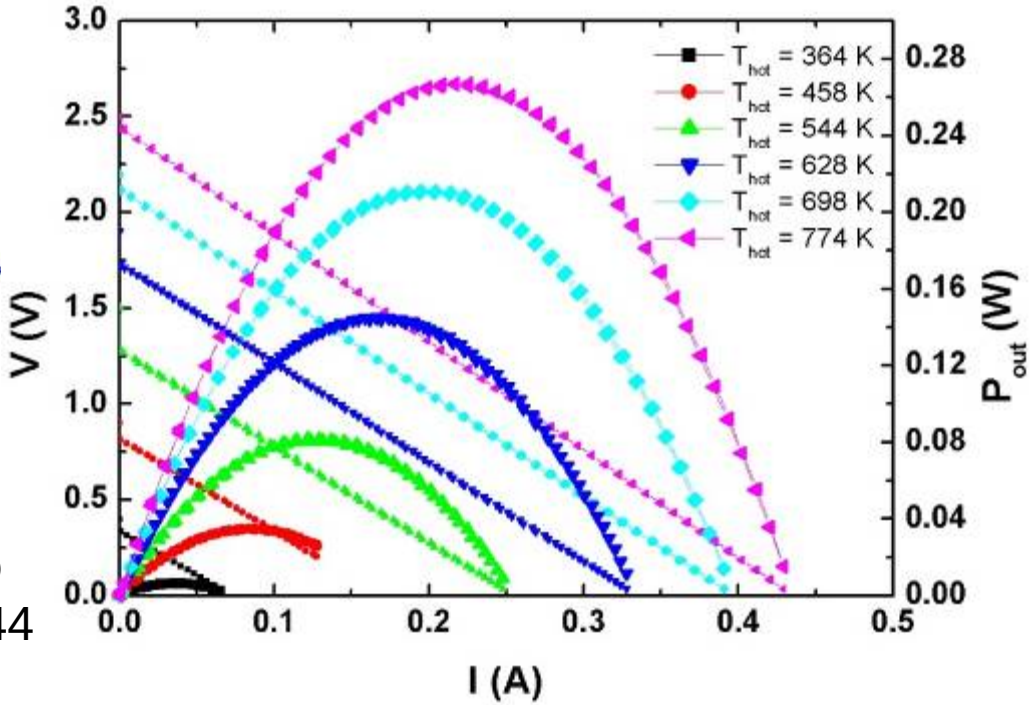

Packing density ~ 60 %.
***P*$_{max}$ from 267 mW (1st generation) to 987 mW (2nd generation),** V_{OC} of ~ 2.44 V at T_{hot} = 774 K.

The power density delivered at operating point for photovoltaic cells made of crystalline Si, crystalline GaAs (~ 25 mW cm^{-2}), poly-Si (~ 20 mW cm^{-2}), CuInGaSe2 (~ 18 mW cm^{-2}), CdTe (~ 16 mW cm^{-2}) and a-Si (~ 13 mW cm^{-2}).

O. Brunko, M. Trottmann, P.Tomes et al

HT Solar converter

Solar Power Concentrator

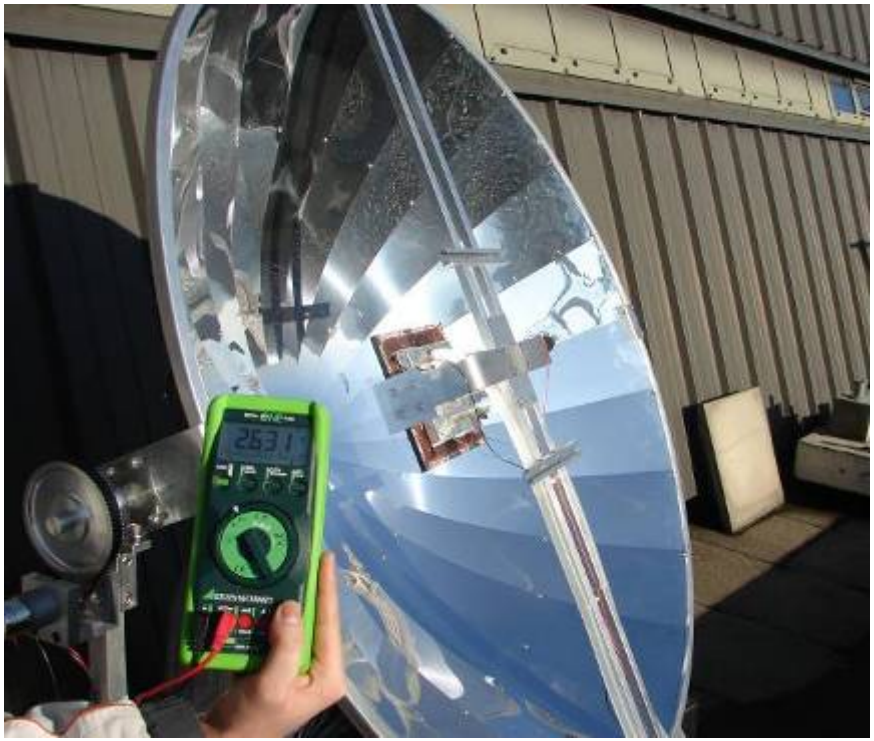

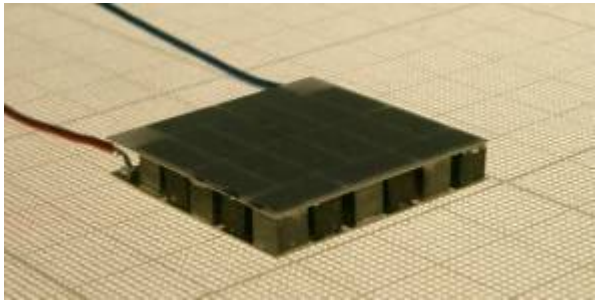

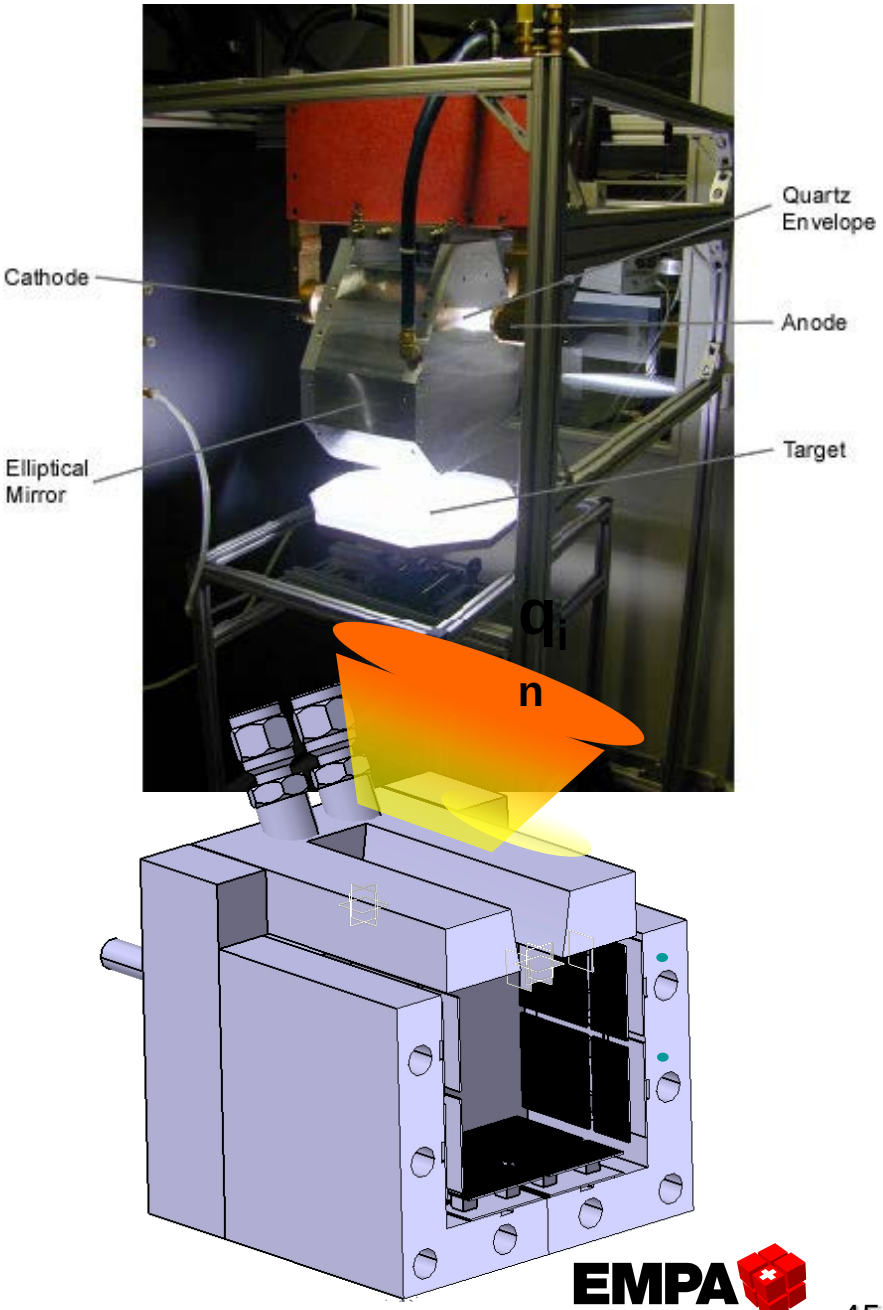

Summary and Outlook

New perovskite-type thermoelectric oxides and photo-electrocatalytic oxynitrides : direct solar energy conversion (hν and kT way):

- ✓ band gap and defect control by innovative synthesis processes
  - ✓ 10 times higher electrode activity
- ✓ large thermopower in correlated electronic systems
  - ✓ Giant Seebeck in $EuTiO_3$ derivates (S>1000 μV/K)
- ✓ low thermal conductivity by hindering phonon transp. on grain boundaries
  - ✓ synthesis method for titanate nanocubes / composites with 3 times lower κ
- ✓ convert concentrated solar radiation.
  - ✓ high T thermoelectric conversion: from 0.2 W to 1 W power output
  - ✓ thermoelectric conversion at T>700°C demonstrated

Interesting candidates: oxynitridefluoride perovskites, doped ZnO, 2D-oxides, nitrides, Heussler compounds, MIT structures, nanoinclusions, nanocomposites

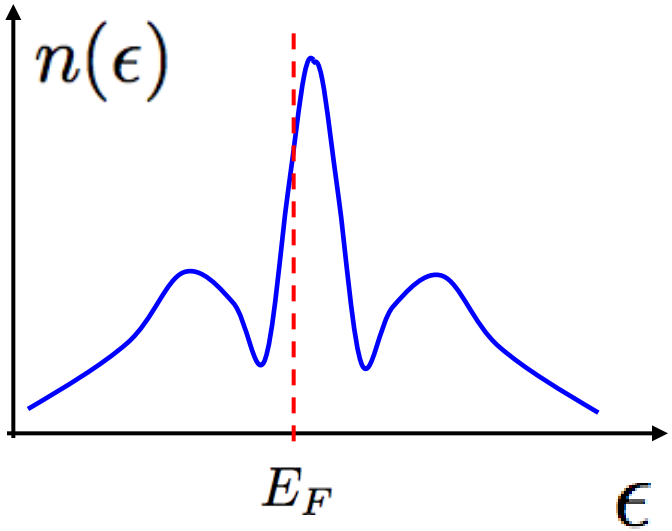

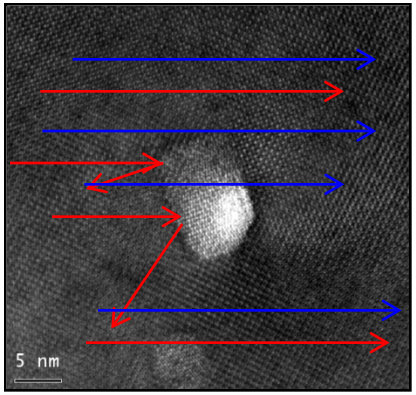

EMPA

Materials Science & Technology

Acknowledgements

- Materials: Andrey Shkabko, Alexandra Maegli, Songhak Yoon, Lassi Karvonen, Leyre Sagarna, Dmitry Logvinovich
- Devices: Matthias Trottmann, Oliver Brunko, Sascha Populoh, Petr Tomes, Celine Leroy, Takashi Hisatomi, Michael Grätzel, EPFL
- FE-simulations: C. Sutter, A. Bitschi, ETHZ
- Funding: Swiss Federal Office of Energy (BfE), Swiss Nat. Sci. Foundation (SNF), DfG, EU 7thFP, KTI
- Beamtime: Swiss Spallation Neutron Source (SINQ), superSTEM, and HASYLAB-DESY

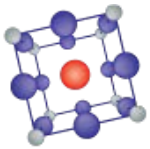

MaNEP
SWITZERLAND

Schweizerische Eidgenossenschaft
Confédération suisse
Confederazione Svizzera
Confederaziun svizra

Swiss Confederation

Swiss Federal Office of Energy SFOE

swisselectric research

EMPA

Trends in TE: heusler, nanostructured and regenerative

Nanostructuring and phase transitions in half heuslers

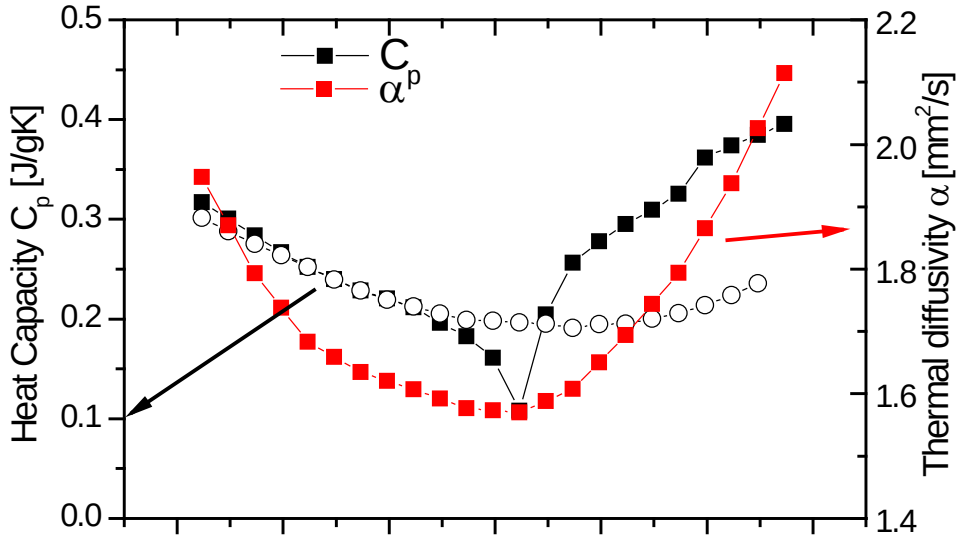

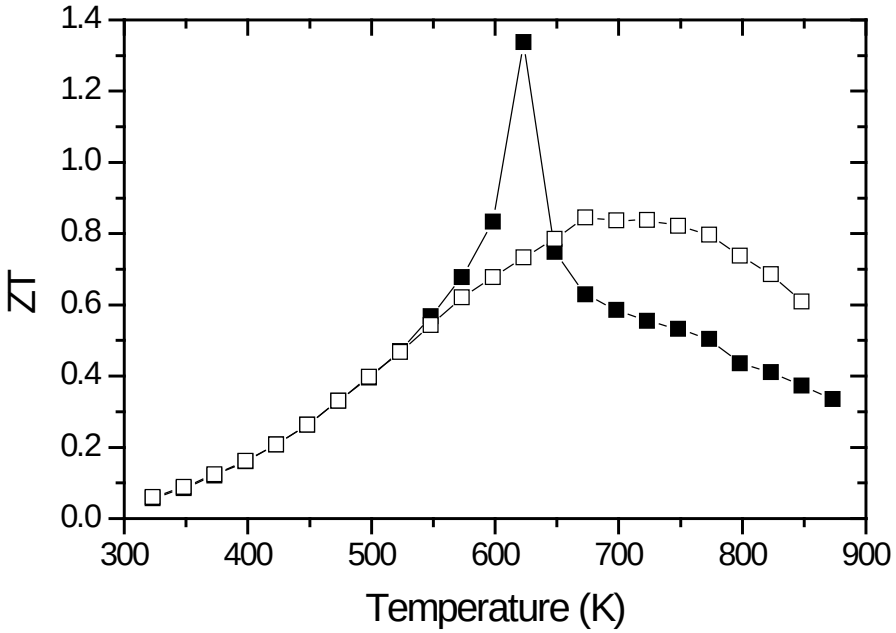

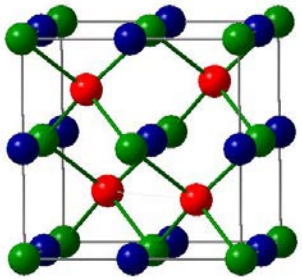

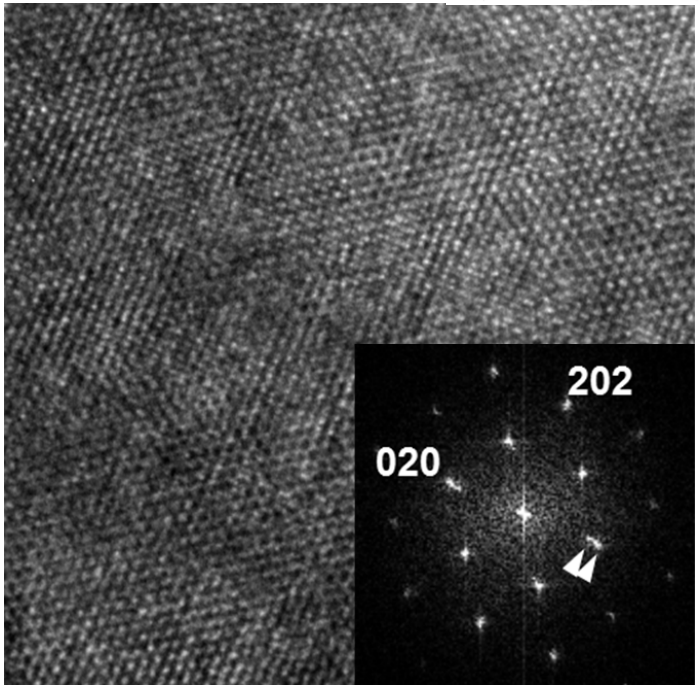

$Ti_{0.37}Zr_{0.37}Hf_{0.26}NiSn$: XRD and HRTEM

S. Populoh, L. Sagarna, et al, Scripta Mat., 66, (2012) 1073–1076.

EMPA
Materials Science & Technology

$(Sr,Eu)Ti_{1-x}Nb_xO_{3+\delta}$ and

Soft chemistry synthesis method for nanostructured titanates

κ from >7 W K^{-1} m^{-1} to <2.5 W K^{-1} m^{-1}

[001] zone axis: image and Fast Fourier Transform-calculated diffraction pattern

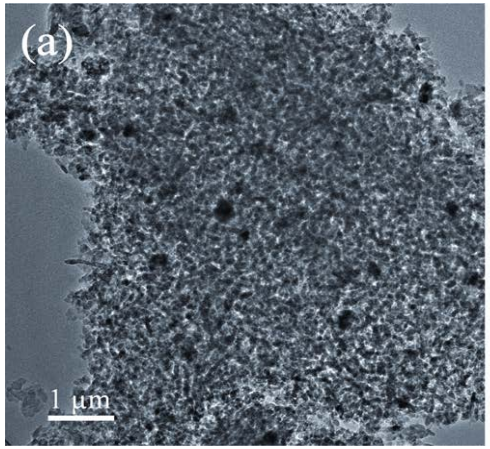

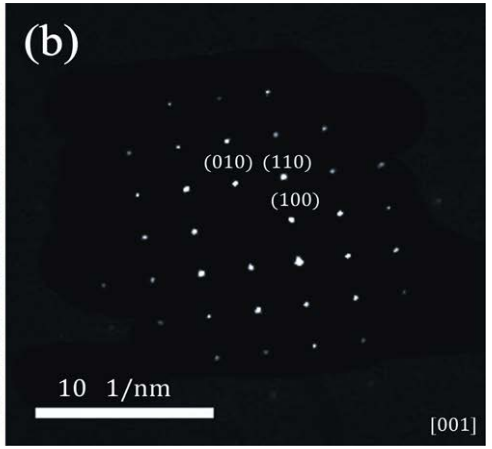

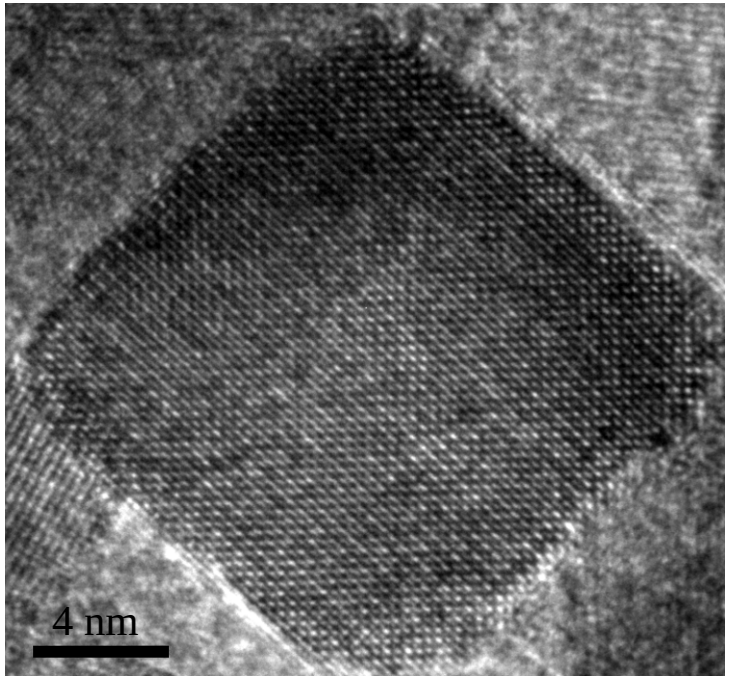

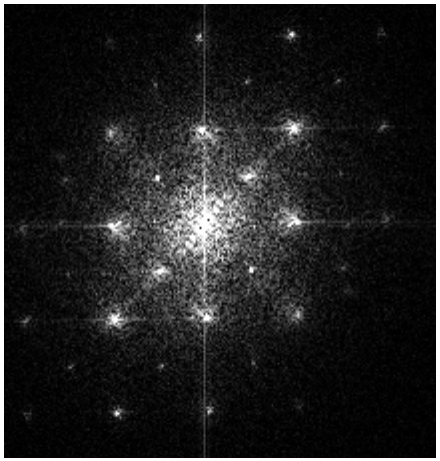

ZT @1000 K in air < 0.1

A. Maegli, L. Sagarna , A. Shkabko et al

EMPA
Materials Science & Technology

Plasma Nitridation of titanates: $EuTi(O,N)_3$

Microwave Induced Plasma Ammonolysis (MIP)

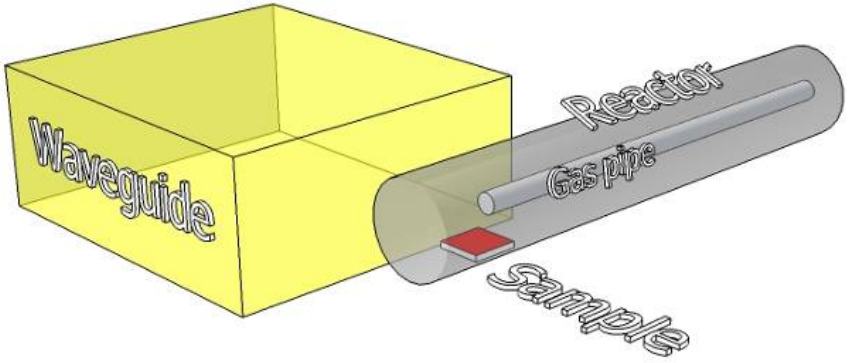

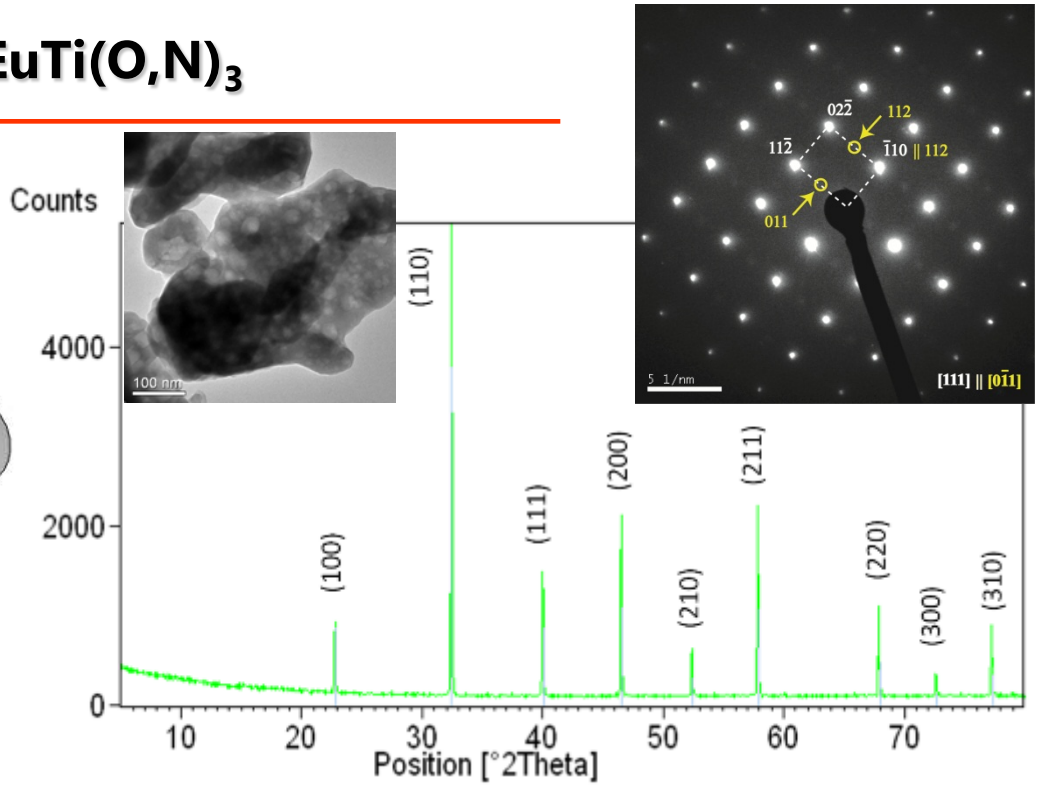

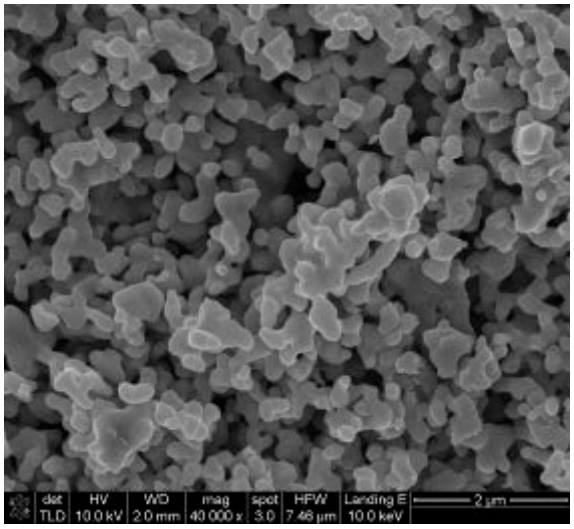

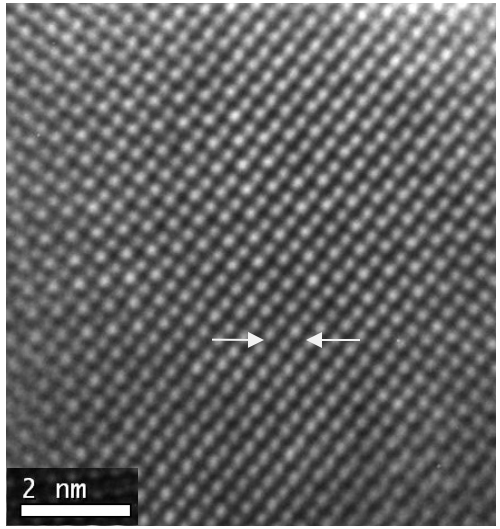

- HR-TEM images, SEM and XRD of $EuTiO_3$:N similar.
  The arrows indicate the size of the cubic unit cell: a≈4 Å
- ND and ED of oxynitride: symmetry lowered to orthorhombic Pnma.
- Low res. TEM: porous particles, not well sintered

Reducing the thermal conductivity

$$ZT = \frac{S^2 \sigma}{\kappa} T$$

$$\kappa_{total} = \kappa_{ph} + \kappa_e$$

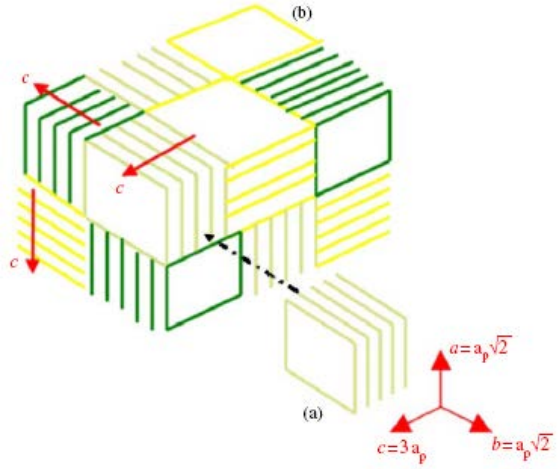

$$\kappa_{ph} \propto C\ \upsilon_S\ \ell_{ph}$$

C : Heat capacity per unit volume
υ_S : Phonon velocity (speed of sound)
ℓ_{ph} : Phonon mean free path

Increasing phonon scattering by:

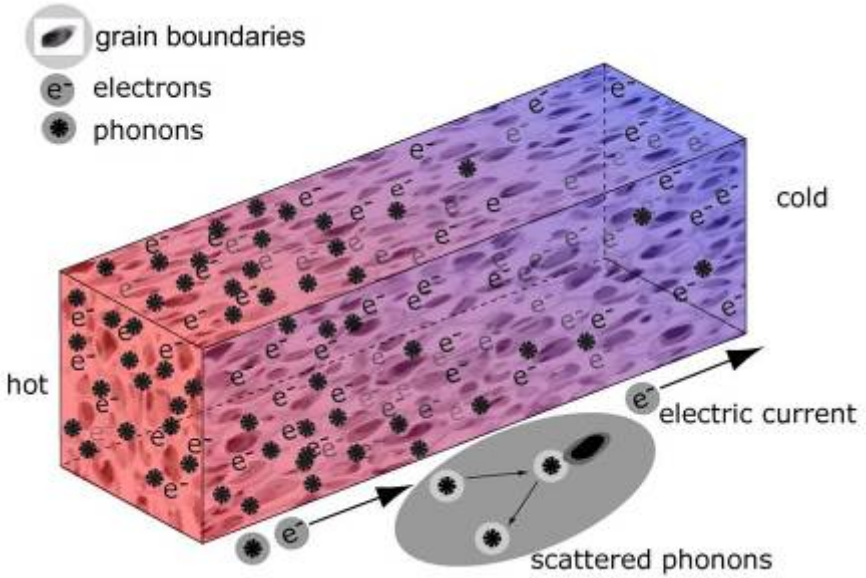

- ➞Grain boundaries scattering (ℓ_{ph})
- ➞Complex crystal structures
- ➞High atomic weight (decreasing of υ_S)
- ➞Crystal defects, domains or pores
- ➞“misfit” structures
- ➞Phase transitions

„phonon glass - electron crystal“